MSc THESIS REPORT

UNVEILING THE EFFECT OF BURREN LOCUS DUPLICATION IN NON-PHOTOCHEMICAL QUENCHING & CYCLIC ELECTRON FLOW

Second half of 2021 - beginning of 2022

Master thesis at Genetics

Jara Jauregui Besó

Registration number: 1044968

MSc Plant Biotechnology (Functional Plant Genomics) Major Thesis (36 ECTS)

Supervision: Louise Logie, Tom Theeuwen & René Boesten

Examiners: René Boesten & Phuong Nguyen Thu Phong

Laboratory of Genetics, Wageningen University & Research

CONTENTS

ACKNOWLEDGEMENTS

For their aid in the realization of this project I would like to thank: Louise Logie and Tom Theeuwen for their mentorship, inspiration, and support; René Boesten for general guidance and help with cloning work as well as Francisca Reyes, David Oomen, Maria Mastoraki and Hedayat Bagheri for the collaboration; Delfi Dorussen for the cooperation in the development of a phenotyping protocol. Special thanks to Konrad Łosinski for helping me carrying out the expression experiments and for being such a supportive friend. Finally, I would like to thank Mark Aarts and the Botanical Genetics group at Wageningen University for welcoming me in the group for the past months and giving me the opportunity to develop myself professionally at the Laboratory of Genetics.

ABBREVIATIONS

ΔΨ: Transmembrane potential difference

ΔpH: H^+ trans-thylakoid gradient

Φ_{PSII}: $\frac{(F_{mp}-F_p)}{F_{mp}}$, maximum efficiency of PSII, photochemical quenching or photochemistry

AL: Actinic Light (photosynthetically active light)

ATP: Adenosine triphosphate

bp: Base pair

Bur-0: Burren-0

Car: Carotenoid, Car* excited state

CEF: Cyclic electron flow

Chl: Chlorophyll (type a Chl_a, type b Chl_b). ^{1}Chl* excited state. ^{3}Chl* ROS forming excited triplets

crr: Chlororespiratory reduction NDH deficient t-DNA mutant

Cyt *b_6f*: Cytochrome *b6f*

dBur: Bur lines with nucleotypic duplication, sBur no nucleotypic duplication

Fd: Ferredoxin

F ': Fluorescence steady state during AL

F_m: Maximum fluorescence parameter without AL, when all P680 are blocked by a saturating pulse

F_m': Maximum fluorescence during AL

F_m'': Fluorescence during AL + SP, after a relaxation period with FR and without AL

F_0: Fluorescence in darkness, optimum photochemical electron transfer capacity of PSII

F_0': Minimum fluorescence value in PIFR

F_p: Maximum fluorescence value in PIFR

FNR: Fd-$NADP^+$ reductase

FR: Far-red light (700 - 750 nm)

H^+: Proton(s)

HL: High Light

hv: Photon energy

KO: Knock-Out

LEF: Linear electron flow

LHCI: Light Harvesting Complex I

LHCII: Light Harvesting Complex II

LL: Low light

NADPH: Nicotinamide adenine dinucleotide phosphate, $NADP^+$ oxidized form

NDH: Respiratory Complex I-like NADPH

ndhO1: NDH defective T-DNA mutant (dysfunctional NdhO subunit)

NPQ: $\frac{F_m}{F_{mp}} - 1$, non-photochemical quenching

OEC: Oxygen evolving complex

PAM: Pulse amplitude modulation / Protospacer Adjacent Motif

PIFR: Post-illumination fluorescence rise

PGR5: Proton Gradient Regulation 5

pgr5: PGR5 deficient mutant

PGRL1: PGR5-Like Photosynthetic Phenotype 1

PC: Plastocyanin

pmf: Proton motive force

PnsL1: Photosynthetic NDH subunit of luminal location 1

PSI: Photosystem I

PSII: Photosystem II

P700: Reaction centre PSI

P680: Reaction centre PSII

PQ: Plastoquinone

ROS: Reactive Oxygen Species

RT- qPCR: Real time quantitative polymerase-chain reaction

sBur: Bur cybrids lacking the nuclear locus duplication

SP: Saturating light pulse

sgRNA: Single-guide RNA

TU: Transcriptional unit

qE: $\frac{F_m}{Fm'} - \frac{F_m}{Fm''}$, fast component of NPQ

qI: $\frac{(F_m - Fm'')}{Fm''}$, photoinhibition NPQ

ABSTRACT

In plants, adapting photosynthesis to constantly changing light environments is crucial to ensure viability. Cyclic electron flow (CEF) can modulate photosynthetic electron transport by increasing the trans-thylakoid proton gradient (ΔpH) that: (1) increases ATP synthesis balancing ATP/NADPH energy budget and (2) activates non-photochemical quenching (NPQ). NPQ is the photoprotective process by which harmful light energy excess is dissipated as heat. Delayed NPQ relaxation upon decreasing light intensity hinders optimum photosynthetic efficiency and thus biomass production. Hence, improving the understanding on how CEF regulates NPQ holds potential for future breeding prospects. The present project focused on characterising the increased NPQ phenotype of two *Arabidopsis thaliana* Burren cybrid lines (paternally derived nucleotype and maternal plasmotype), with a nuclear locus duplication: $dBur^{Bur}$ and $dBur^{C24}$ ("double"-$nucleotype^{plasmotype}$). Duplicated *PnsL1* was studied as candidate gene for the phenotype, as it is part of the NAD(P)H dehydrogenase-like complex (NDH) that regulates one of the main CEF pathways in Angiosperms. First, analysis of antecedent dBur phenotypic data showed that upon long subjection to fluctuating light, the duplication had increasing effects on NPQ at 500 μmol photons m^{-2} s^{-1} but did not have any distinctive impact upon higher light intensities (1000 μmol photons m^{-2} s^{-1}). Under constant lower light intensities (200 μmol photons m^{-2} s^{-1}) the duplication was found to decrease NPQ. Additionally, it was discovered that dBur phenotype was also plasmotype dependent. Decreasing Bur plasmotype effects in NPQ (relative to C24) were found to be relevant at 200 μmol photons m^{-2} s^{-1} and independent from the duplication. Second, to evaluate the implication of *PnsL1* in the dBur phenotype over-expression of the candidate gene was verified via real-time quantitative PCR (RT-qPCR), also proving that *PnsL1* expression is not regulated by increase in light intensity. Cloning of CRISPR/Cas9 knock-out (KO) constructs was also attempted. Third, to assess whether distinctive dBur phenotype could be explained by increased NDH activity, NPQ and NDH activity were measured in plants receiving constant (200 μmol photons m^{-2} s^{-1}) and fluctuating light treatment. When the light intensity used for fluorescence measurements was rapidly shifted (from 200 to 1000 μmol photons m^{-2} s^{-1}) the duplication resulted in NPQ decrease with a concomitant increase in efficiency of Photosystem II (Φ_{PSII}). These differences were linked to increased NDH activity owing to locus duplication, which was detected for $dBur^{C24}$ only. Altogether, this study provides a comprehensive characterisation of the dBur photosynthetic phenotype that sets the basis for future research on *PnsL1* over-expressing and KO lines.

1. INTRODUCTION

"Our planet is alive and photosynthesis powers it"[1]. Life endurance and proliferation depend on the constant influx of energy driven by photosynthesis, a complex system by which plants, algae or cyanobacteria capture sunlight's energy held in photons and stabilize it, forming the chemical bonds that constitute the foundation of living matter.

In plants, photosynthetic energy conversion efficiency is one of the main factors determining growth[2]. Yield is in fact correlated to photosynthesis[3], and thus fine-tuning it is an attractive approach to increase agricultural output. In the recent years, engineering photosynthesis in crops has become a popular strategy to meet the raising food demand[2,4–7]. Different modes of action have been suggested to achieve this goal. A reasonable possibility consists in modifying photoprotection[3,8,9], a series of mechanisms by which photosynthetic processes are halted upon damaging, high light irradiance. Because plants are exposed to constantly fluctuating light environments, fast adaptation to different light conditions is crucial. Slow adjustment of photoprotective machinery to transitions from shade to sun hampers this acclimation, and it is estimated to reduce photosynthetic biomass formation up to 30%[10–12]. Kromdijk *et al.*[8] showed in *Nicotiana tabacum* that accelerating induction and relaxation of photoprotective systems under fluctuating light can result in an up to 15% increase in dry matter production. However, another study was unsuccessful to replicate this effect in *Arabidopsis thaliana*[13]. The reality is that the molecular mechanisms involved in photoprotection are still poorly understood. Before considering its manipulation as a feasible strategy, further research is essential to unveil its regulation and functioning within photosynthesis as a whole.

Photosynthesis altogether is a complex biological process run by two key mechanisms: i) the light reactions, in which via oxidation of water into oxygen, light energy is converted into chemical energy and reduction power – adenosine triphosphate (ATP) and nicotinamide adenine dinucleotide phosphate (NADPH) respectively; and ii) the Calvin-Benson cycle, where ATP and NADPH are used to reduce atmospheric CO_2 and form sugars[1]. These reactions occur in chloroplasts – specialized organelles formed by membranes arranged into vesicles called thylakoids – and the stroma, the surrounding aqueous phase. Light reactions happen in the thylakoid membranes, whereas carbon fixation takes place in the stroma. Four protein supercomplexes comprise the photosynthetic machinery in the thylakoid membrane: Photosystem II (PSII), Cytochrome (Cyt) *b6f*, Photosystem I (PSI), and the ATP synthase (*Figure 1*)[14].

Both PSII and PSI capture photonic energy by their corresponding Light Harvesting Complexes (LHCII, LHCI). These are composed by aggregates of homologous proteins and pigments such as chlorophylls (Chl) and carotenoids (Car). When collecting light energy, Car and Chl chromophores, absorb light and form excited states (Car*, ^{1}Chl*) that transfer energy towards the reaction centres of PSII and PSI, P680 and P700 respectively [15]. Consequently, a high energy electron is boosted in the reaction centres, which is then transmitted through the main protein complexes in a series of redox reactions that drive ATP and NADPH synthesis. This can occur via two divergent pathways (*Figure 1*). The majoritarian one is called Linear Electron Flow (LEF). In LEF electrons are captured by PSII and transferred in a linear fashion to the rest of the chain components until they reach the $NADP^+$ reductase (FNR, associated to Cyt *b6f*), resulting in NADPH formation. In the process, protons (H^+) accumulate in the lumen forming a H^+ trans-thylakoid gradient (ΔpH). Together with the transmembrane potential difference (ΔΨ), they generate the proton motive force (*pmf*). *pmf* triggers ATP synthase to pump H^+ back to the stroma driving ATP formation (*Figure 1*)[15,16]. Overall, for 8 absorbed photons (*hv*), LEF results in the lumenal accumulation of 12 H^+ and a 1.28 ATP/NADPH production ratio[17]. An alternative system exists that involves the repeated cycling of electrons through PSI only, known as cyclic electron flow (CEF). After leaving PSI, some electrons go back to the plastoquinone pool (PQ) and return to PSI recurringly. The loop promotes lumenal accumulation of H^+ that increases ATP formation. However, because electrons are diverted from $NADPH^+$ reductase, NADPH formation does not occur[18,19] (*Figure 1*). Therefore, CEF

activity results in the increase of ATP/NADPH production ratio (up to 1.5 ATP/NADPH in C3 plants)[17]. The specific purpose of CEF in photosynthesis remains a mystery and its regulation is still not fully comprehended[20]. Two primary functions are assumed: i) Additional ATP synthesis to balance the deficient LEF ATP/NADPH production ratio needed for the Calvin-Benson cycle[17,21,22]; and ii) Regulation of light capture under excessive light conditions, playing a photoprotective role[18,19,23,24].

Safe and efficient operation of PSII and PSI photoreactions highly depends on the amount of light absorbed by plants throughout the day[25]. Due to diurnal variations, leaves are often exposed to an excessive light energy supply. Under strong illumination, photosynthesis becomes limited due to saturation of the Calvin-Benson cycle leading to the static reduction of the preceding electron carriers[18]. In result, the thylakoid membranes overload with electrons[26–28]. PSII is relatively slower than PSI transmitting excited electrons and, for this reason, it is particularly prone to photoinhibition[29]. This phenomenon occurs when, because of light excess, over-excited Chl triplets (^{3}Chl*) accumulate in PSII. ^{3}Chl* react with O_2, forming reactive oxygen species (ROS) that damage thylakoid membranes and degrade a key component of P680, the core D1 protein. This leads to the inactivation of PSII[30–32].

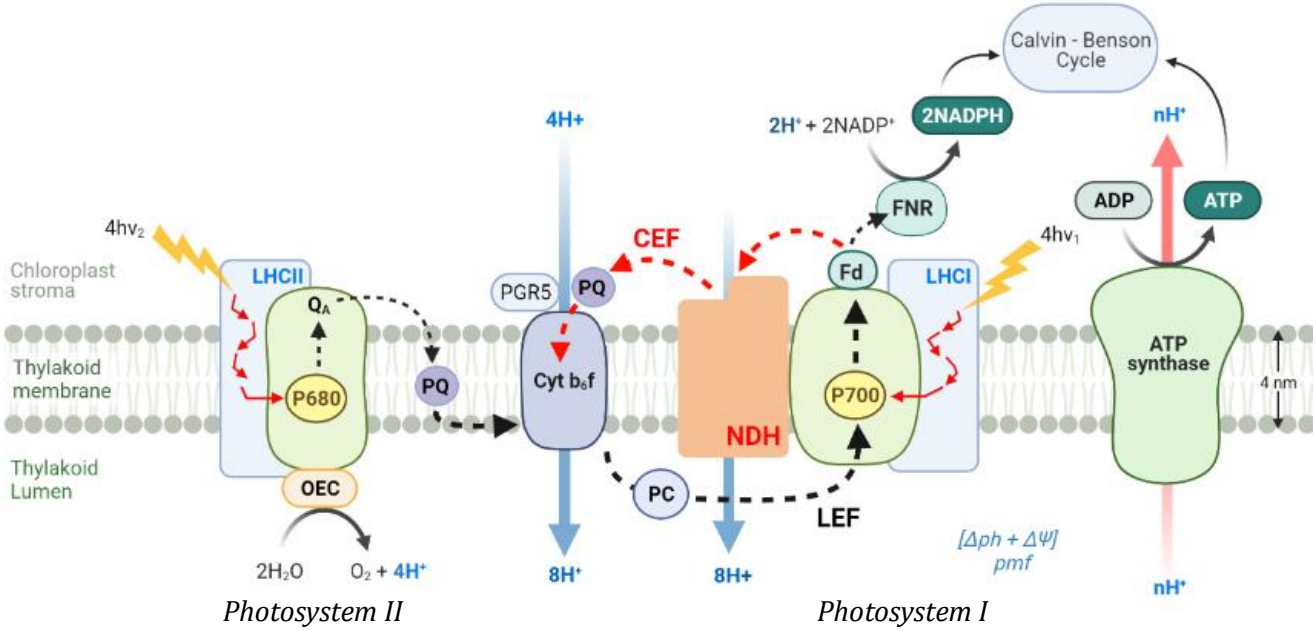

***Figure 1* | Diagram of the photosynthetic light reactions occurring in the thylakoid membrane of Plants.** Five major protein complexes are shown, from left to right: Photosystem II, (PSII; water-plastoquinone oxido-reductase), cytochrome (Cyt) b_6f (plastoquinol-plastocyanin-oxidoreductase), NDH (NAD(P)H deshydrogenase-like complex I), Photosystem I (PSI; plastocyanin-ferredoxin-oxido-reductase) and ATP synthase. Photonic energy (*hv*) absorption in both PS by their light harvesting complexes (LHC) leads to excitation of electrons in their reaction centres, P680 and P700. In PSII, high-energy electron is passed to an acceptor plastoquinone (PQ)– Q_A; then, H_20 is oxidized in the oxygen-evolving complex (OEC). The freed electron is sequestered to PSII as a replacement of the one previously removed. O_2 is generated in the process, and protons (H^+) are released in the thylakoid lumen. The PQ pool transmit the light-energized electron to the Cyt *b6f* complex, that donates it to the plastocyanin (PC) by pumping H^+ into the luminal space[1,15,16]. Simultaneously, photon energy (*hv*) is used in PSI reaction centre (P700) to excite another high-energy electron, passed via ferredoxin (Fd) to Fd-$NADP^+$ reductase (FNR), which transfers the electrons to $NADP^+$ resulting in the formation of NADPH. PSI replaces lost electrons by receiving the ones released in PSII from PC. In the process, H^+ accumulate in the lumen forming a H^+ trans-thylakoid gradient (ΔpH). Together with the transmembrane potential difference (ΔΨ), they generate the proton motive force (*pmf*). *pmf* triggers ATP synthase to pump H^+ back to the stroma driving ATP formation. The present electron movement between PSII and PSI resulting in ATP and NADPH synthesis is named linear electron flow (LEF) [15,16]. An alternative system exists that involves the repeated cycling of electrons through PSI only, known as cyclic electron flow (CEF). After leaving PSI, some electrons go back from Fd to the PQ pool, pass through the Cyt *b6f* complex and return to PSI recurringly. The loop promotes the H^+ gradient driving ATP synthesis as usual. However, because electrons are diverted from $NADPH^+$ reductase, NADPH formation does not occur[18,19]. In Angiosperms, CEF is known to operate through PGRL1/PGRL5 (PGR5) and NDH-mediated pathways. The stoichiometry of the depicted reactions corresponds to four electrons.

To prevent PSII photoinhibition, CEF rate rises to ensure that the electron flow continues, enabling the oxidation of the electron carriers in the chain[18]. Consequently H^+ import to the lumen increases, which generates a large proton gradient that activates the non-photochemical quenching (NPQ) within the antenna. NPQ is a photoprotective mechanism by which LHCII detach from PSII to protect it, halting electron transfer and quenching the energy surplus as heat[17,18,33]. Its purpose is to maintain the PQ pool optimally oxidized under excessive light conditions and thereby protect PSII and PSI from over-reduction[34]. NPQ altogether is an intricate process. It involves different steps driving the conformational change of LHCII from an unquenched to a quenched state, known as NPQ components. The main NPQ component, qE (fast component of NPQ), refers to this detachment of the major LHCII proteins to form quenching aggregates. It is triggered by the increase of trans-thylakoid ΔpH when H^+ accumulate in the lumen due to light excess, and relaxes in a time window of 1-5 minutes[33,35–37]. Another relevant NPQ component refers to the photoinhibitory quenching driven by D1 photoinactivation, named qI. It is a slow component, relaxation (repair) occurs within hours or longer[38,39].

Even though they can be rapid, changes in NPQ are not capable of adapting to fluctuations in irradiance absorption immediately. Relaxation of NPQ occurs at a slower rate than induction, especially after exposure to excessive light during extended or repeated periods[8,40]. The delayed restoration of LHCII to unquenched state impedes efficient capture of light, which leads to a transient reduction of photosynthetic CO_2 fixation and in turn biomass accumulation[10–12]. It is for this reason that understanding the regulation of NPQ induction and relaxation is crucial to conceive achievable methods of manipulation.

In 2020 Flood and Theeuwen published their work on the effect of variable organellar genomes on the phenotype[41]. In the study, they crossed seven *A. thaliana* accessions to make cybrids[42] – lines with maternally derived plasmotype (mitochondrial and chloroplast DNA) and paternal nucleotype (nuclear DNA) – in all possible combinations. To develop them they made use of *GFP-tailswap*[42,43] maternal haploid inducers, which pollinated with a WT plant produce haploid offspring containing solely paternal nuclear genes. Via genome duplication or restitutional meiosis double haploids are formed in the next

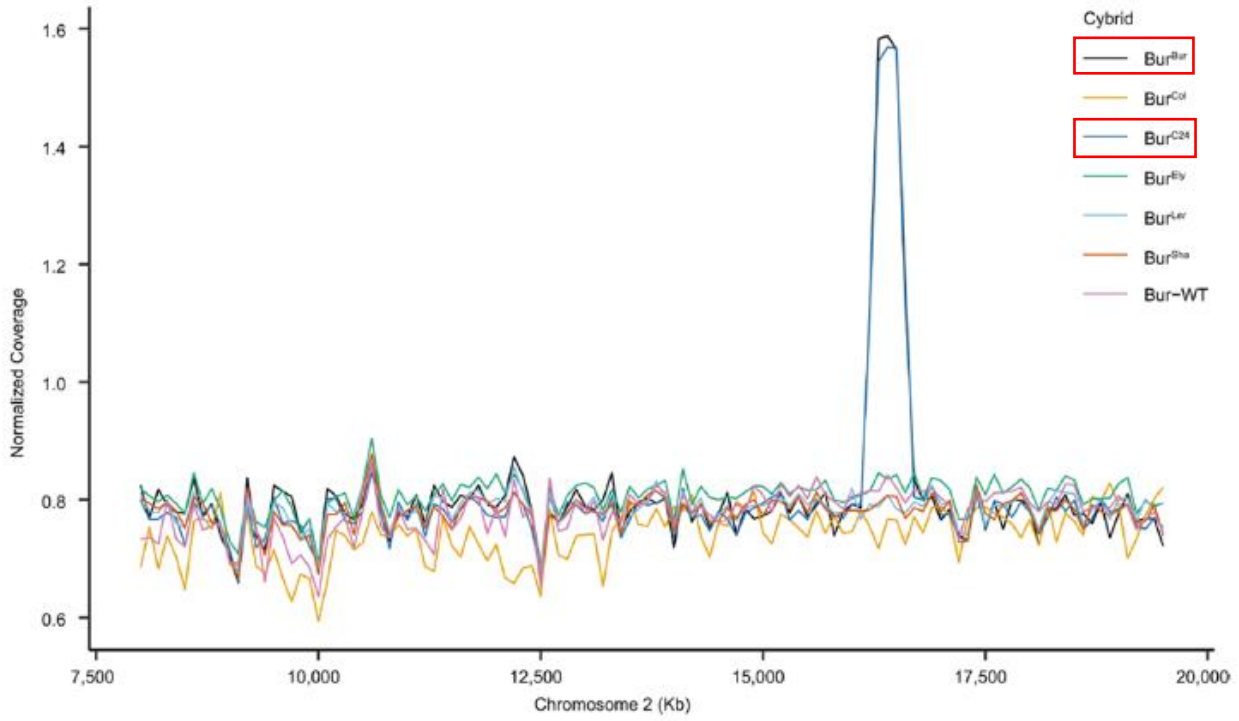

***Figure 2* | Coverage plot depicting the duplication found on chromosome 2 in dBur^{Bur} and dBur^{C24}.** Normalised read coverage of the chromosome 2 7.500 – 20.000 bp region for Bur-WT and six other Bur cybrids is shown. Plot exhibits the spontaneous nuclear DNA locus duplication found in dBur^{Bur} and dBur^{C24} (marked in red), probably inherited from the same Bur-WT parental nucleus donor. Figure obtained from the Extended Data section in [41], edited.

generation, the cybrids[43]. The generated lines were screened for several phenotypic trait performance under stable and fluctuating light in the Dynamic Environmental Photosynthetic Imaging (DEPI) system in Michigan State University[44]. Within the evaluated panel, two cybrid Burren (Bur) lines stood out for their increased NPQ: Bur^{Bur} and Bur^{C24} ($nucleotype^{plasmotype}$). However, these plants had to be excluded from the study, as they were found to have the same *de novo* nucleotypic locus duplication, likely originated in one of the Bur-WT paternal donors[41]. The DNA duplication was detected in chromosome 2 –from 16200 to 16700kb approximately (*Figure 2*). Through short-read DNA sequencing and RNA sequencing assays, a total of 83 genes belonging to this region were identified to be duplicated.

A duplication can consist of an extra copy of the entire genome (whole-genome duplication) or only one or a few genes (small-scale duplication)[45]. There are several consequences to this phenomenon, although generally the immediate effect of gene duplication involves an increase in gene dosage. This increase can, in some circumstances, enlarge the amount of gene expression implying changes on the phenotype[46]. Among the genes present in the duplication of Bur cybrids – from now referred to as $dBur^{C24}$ and $dBur^{Bur}$ ("duplicated"-$nucleotype^{plasmotype}$) – one gene involved in CEF was found: *Photosynthetic NDH subunit of Lumenal location 1* (*PnsL1*, AT2G39470). This discovery led to hypothesize that CEF could be the leading cause promoting increased NPQ induction in Bur cybrids containing the duplication (dBur), and that *PnsL1* may be a logical candidate to be responsible for this phenotype.

NDH (chloroplast NAD(P)H dehydrogenase-like) is a chloroplastic protein complex with H^+ pump activity that drives one of the two CEF pathways known to function in Angiosperms (*Figure 1*)[47,48]. The predominant one is known as the PGR5-PGRL1 protein pathway, whereas the one operating through NDH complex is minor[49,50]. Nevertheless, NDH is regarded as more energetically efficient, as it transfers two times more H^+ per electron through the thylakoid membrane[17,49]. Both PSI cyclic pathways transfer electrons to the PQ pool by boosting H^+ import to the lumen, thereby contributing to *pmf* formation and increase in ΔpH[49].

The NDH must be coupled with PSI in order to fulfil its function in CEF[48,51]. It is known to interact with PSI via Lhca5 and Lhca6, two linker proteins that belong to the LHCI[51]. They are essential to mediate the association of NDH with two different copies of LHCI-PSI, allowing NDH-PSI supercomplex formation (*Figure 3*)[48,51,52]. NDH in Arabidopsis contains at least 30 subunits, 11 of them are encoded in the chloroplast, whereas the rest – PnsL1 included – are encoded by nuclear genes (*Figure 3*)[47,50,53]. PnsL1

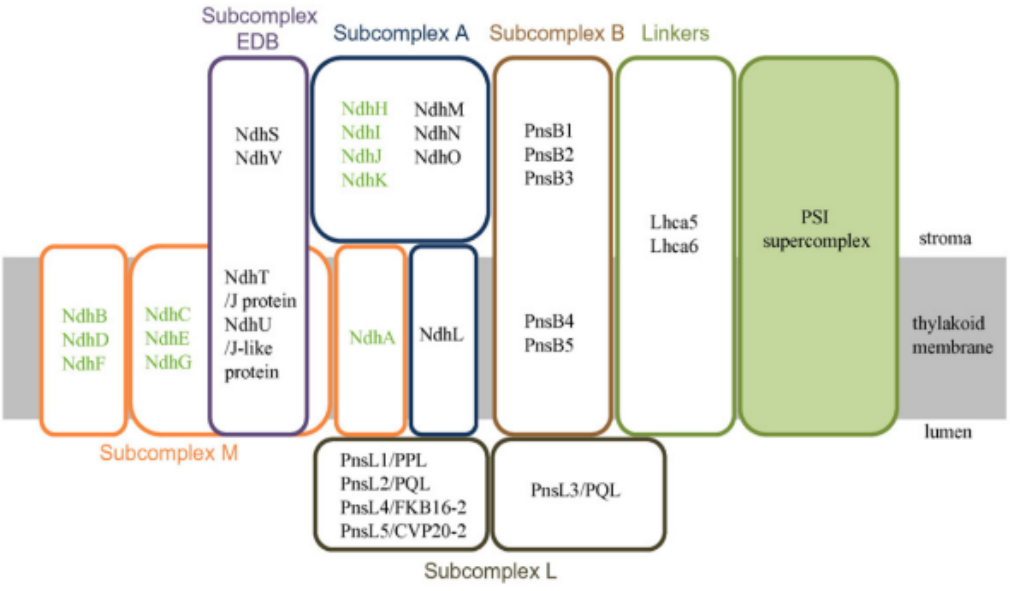

Figure 3 | Schematic model of the NDH-PSI supercomplex in *Arabidopsis*. Subunit locations are based on protein stability in mutant backgrounds and do not correspond to real positions in the 3D structure. Green letters represent plasmid-encoded subunits. From[46].

is part of the L subcomplex located in the lumenal side of the thylakoid membrane[47,54]. It may have a structural function by stabilizing the NDH-PSI supercomplex[51]. In fact, *PnsL1* has been found to be highly co-expressed not only with other NDH subunits, but also with *Lhca6*[51,54]. It also has been proven to be essential for the interaction of NDH complex with Lhca5[52]. Studies using Arabidopsis *pnsl1* mutants show that it is indispensable for NDH accumulation in the thylakoid membranes[55], as well as for the correct functioning of the complex, since lack of PnsL1 results in impaired NDH activity[54].

Because of its function in the NDH complex, it could be possible that PnsL1 is involved in CEF dependent NPQ regulation. Understanding NPQ regulation, as previously indicated, holds potential for future breeding efforts to boost crop yield through improvement of photosynthesis. The presence of the nuclear locus duplication causes an apparent NPQ increase in dBur cybrids. These phenotypic alterations might, presumably, be attributed to increased *PnsL1* expression. Studying how *PnsL1* duplication can alter NPQ may contribute to a better comprehension of both *PnsL1* function and NPQ regulation, which might lead to novel approaches for manipulation. To that end, the present MSc thesis project focused on resolving three major research questions: first, determining how and under which conditions dBur NPQ and photosynthetic phenotype is altered due to duplication; second, finding if this trait can be explained by increased *PnsL1* expression; and third, whether the distinctive photosynthetic phenotype might be driven by increased NDH dependent CEF.

To characterise the NPQ and photosynthetic phenotype of dBur in detail, the unpublished data from Flood and Theeuwen's study[41] involving dBur cybrids was analysed. Two datasets containing time-series measurements of photosynthetic parameters were examined. These contained information collected during 3 days of constant, sinusoidal and fluctuating light. The aim was to gain more understanding on the time subjected shifts in NPQ depending on the light conditions. Then, in order to enable further assessment of the potential role of the *PnsL1* in the dBur phenotype, expression of *PnsL1* was quantified under constant and sinusoidal light. Additionally, generation of CRISPR-Cas9 Knock-Out (KO) constructs was attempted. Lastly, to determine whether distinctive NPQ dBur phenotype could be linked to increased NDH dependent CEF, phenotyping experiments were conducted to measure NPQ and NDH activity under constant and fluctuating light conditions. On the first place, these experiments focused on assessing whether the NPQ phenotype detected in the DEPI could be induced in our facilities. To conclude, NDH activity was evaluated to discern whether it could be linked to the NPQ phenotype.

2. MATERIALS AND METHODS

2.1 Plant material

Arabidopsis thaliana WT, cybrid and NDH mutant plants with the following genotypes were included on the experiments. With Burren nuclear background: Bur-0 (Bur-WT, CS76105), dBur^{C24}, dBur^{Bur}, sBur^{Bur} and sBur^{C24} [41]. Columbia background: Col-0 (CS76113), *crr2-2 (chlororespiratory reduction 2*)[56], *ndhO1* (SALK_068922) and *pnsl1* (SALK_063049).

Seeds were cold stratified at 4 °C for four days in 60 mm x 15 Petri dishes containing filter paper soaked with 0.6 mL of demi water. On the fifth day dishes were transferred to a climate chamber at 22 °C with 16/8 h light cycle and kept during 24h to trigger germination. Seeds were sown in rockwool blocks (4 cm^3) soaked in Hyponex growth mix solution (Unifarm). Rubber covers containing a hole in the centre were placed on top to prevent algae from growing around the seedlings. Transparent pipette tips were used to fix the covers to the rockwool.

Plants were distributed following a randomized design in blocks of 4 x 5 and grown in the "Fluctor" (C14, Klima) climate chamber of Wageningen University. This chamber contains a programmable light system that enables growing plants under the desired light setting, such as constant low light or fluctuating light. Light conditions varied per experiment and are specified in their corresponding sections. General growth conditions included 70% humidity, 20/18°C day/night temperature and watering twice a week with Hyponex solution.

2.2 Analysis of the dBur unpublished DEPI data

With the aim of gaining more understanding on the effect of the locus duplication and the Bur plasmotype in photosynthetic performance, the unpublished data generated in Flood & Theeuwen's study[41] involving dBur cybrids was analysed. Results from two different experiments were combined in a single dataset, gathering values belonging to the first three days of the DEPI system[44] (*Supplementary Figure 1*), measured in Michigan State University facilities. The file consisted of time subjected records of Φ_{PSII}, NPQ, qE and qI parameters, collected during 12h long days. Datapoints referred to measurements acquired at the end of every hour of the first day ("flat" or constant light, 200 µmol photons m^{-2} s^{-1}), every half hour in the second (sinusoidal light, maximum intensity 500 µmol photons m^{-2} s^{-1}) and four times per hour in the third (fluctuating light, peak at 1000 µmol photons m^{-2} s^{-1}). Fluorescence values belonging to fluctuating light conditions related to LL and HL periods, of 20 and 8 minutes each. Experiments were conducted in 3-week-old plants grown in constant light conditions (200 µmol photons m^{-2} s^{-1}), transferred to the DEPI facility 24h prior phenotyping measurements.

When these experiments were conducted, Bur^{Bur} and Bur^{C24} cybrids lacking the nucleus locus duplication (sBur) were yet not available. Bur-WT (n = 8) was chosen as control genotype to compare to dBur^{Bur} (n = 7). Bur^{Col} was selected as reference cybrid for dBur^{C24} (n = 8). C24 ad Col plasmotypes have shown to have no significantly different effects in photosynthetic traits[41], hence Bur^{Col} cybrid was regarded as most appropriate option to study the duplication effect.

Two different statistical models were designed to investigate the diversity of genotype, locus copy number and plasmotype effects. They were used to infer best linear unbiased estimations (BLUE) in a mixed model context[57], with the experiment effects treated as random. One model included the genotype as fixed effects only (*Equation* 1), whereas the other one was designed to explore the plasmotype and copy number effect as well as their interaction (*Equation 2*).

$$\underline{Y} = Genotype + \underline{Experiment} + \underline{\varepsilon} \qquad \textit{(Equation 1)}$$

$$\underline{Y} = Copy\ nr. + Plasmotype + Copy\ nr. \times Plasmotype + \underline{Experiment} + \underline{\varepsilon}$$

(Equation 2)

Estimates of the variance components were generated by Restricted Maximum Likelihood (REML) method[58]. The models were run making use of the lme4 package in R[59]. Estimated marginal means computed with the emmeans package[60] were used to deduce effect sizes as relative difference percentage – (a/b – 1) x 100. Genotype comparisons were done for $dBur^{Bur}$/Bur-WT and $dBur^{C24}$/Bur^{Col}, whereas duplication and plasmotypic effect sizes were evaluated as 2 Copy nr./1 Copy nr. and C24/Bur.

2.3 Evaluation of *PnsL1* expression in Bur

Confirmation of the increased *PnsL1* expression in dBur cybrids was done in Bur nucleotype plants with and without nucleus duplication (n = 8). These were grown in constant light (200 µmol photons m^{-2} s^{-1}) for 19 days in 16/8 h day/night cycle, before receiving sinusoidal light treatment half day. Each biological replicate was sampled twice before and after light treatment, 30 minutes after the middle of the light period (8:30 h) when light intensity was 200 and 500 µmol photons m^{-2} s^{-1}, respectively.

Samples contained ~1 cm^2 of fresh leaf tissue that was instantly frozen in liquid nitrogen after removal. Frozen plant material was grinded using glass beads of 2 and 3 mm with the help of a bead mill. Extraction of total RNA was conducted by means of the Direct-zol RNA Miniprep Plus Kit (Zymo-Research) according to manufacturer's instructions. cDNA was directly synthesized from total RNA making use of the SensiFAST cDNA Synthesis Kit (Meridian Bioscience). Reaction was carried out in a final volume of 20 µL containing 4 µL of TransAmp™ buffer, 1 µL of reverse-transcriptase enzyme and 1 µg of RNA template. Complete reaction mix was incubated during 5 minutes at 25 °C, followed by 30 minutes at 42°C and 5 minutes at 85°C. cDNA was diluted 10x before proceeding with quantification.

Real time quantitative polymerase-chain reaction (RT-qPCR) was performed in a Bio-Rad CFX96 Real-Time PCR Detection System using SensiFAST SYBR® No-ROX One-Step Kit (Meridian Bioscience) in a total volume of 10 µL including cDNA template (3µM) and primers (3µM). Target *PnsL1* gene PCR primers (5'-AGCTACTCGCCTTTTGTGGA-3' and 5'-GTGCCCTGAAGTCAAATTCC-3') were designed for 80-120 bp fragment amplification covering exon-exon junctions, with 59-61°C melting temperature (94.4% tested efficiency). RNA processing factor 3 (*RPF3* or PPR, AT1G62930) was selected as reference gene and sequences (5'-AGGGCACGCCTTAGAGATGG-3' and 5'- TGCAATCACAAGGGAAGATGG-3') were obtained from[61] (99.6% tested efficiency). The qRT-PCR conditions were as follows: 3 minutes pre-denaturation at 95 °C, followed by 40 cycles of denaturation at 95 °C for 10 sec + annealing at 60 °C for 15 seconds + extension 72 °C for 23 seconds, ending with a melting curve from 55 – 95 °C for 5 seconds.

Analysis of obtained Ct values was conducted according to Livak & Schmittgen's $2^{-\Delta\Delta Ct}$ method[62], in which the target gene expression is estimated by calculating the base 2 logarithm ($2^{-\Delta Ct}$) of the Ct difference respect to the reference gene ($\Delta Ct = Ct_{target} - Ct_{ref}$). $2^{-\Delta Ct}$ was then used to calculate the gene expression relative to Bur-WT $2^{-\Delta Ct}$ geometric mean ($2^{-\Delta\Delta Ct}$). Relative expression of *PnsL1* was inferred in "constant" and "sinusoidal" sample sets per separate. Additionally, in order to study the expression fold change before- and after-light treatment, $2^{-\Delta\Delta Ct}$ values were deduced by relativisation to own $2^{-\Delta Ct}$ estimates prior to sinusoidal light application. Statistical analysis was performed using single $2^{-\Delta Ct}$ values per sample, applying analysis of variance (ANOVA) in each treatment and two-sample t-test to compare expression before and after treatment.

2.4 Cloning of *PnsL1* Knock-Out constructs

Cloning of CRISPR/Cas9[63] Knock-Out (KO) vectors was conducted via Golden Gate Assembly[64] with the purpose of studying the effect of *PnsL1* function loss in Bur. The goal was to obtain two different types of constructs. One containing two single guide RNA sequences (sgRNA) to ensure complete lack of *Pnsl1* expression in all Bur plants. The second encasing solely one sgRNA, so as to KO only one of the two gene copies in the dBur cybrids.

20 nucleotide guide sequences were generated based on the *PnsL1* coding sequence (AT2G39470), targeting the first or the second exon. CRISPOR.org[65] (http://crispor.org) web tool was used for the guide RNA sequence design, introducing the respective exon sequence, selecting *A. thaliana* as reference genome and *Streptococcus pyogenes* Cas9 (spCas9) as Protospacer Adjacent Motif (PAM). Oligos with the highest specificity scores downstream to the PAM sequence (NGG) were selected, accounting for possible off-targets. All guide sequences with best predicted efficiency targeted the non-coding complementary DNA strand. Reverse complement sequences located in the coding DNA strand were generated using the https://www.bioinformatics.org/sms/rev_comp.html tool. Selected oligos were then matched against whole genome sequencing data containing information on Bur allelic variants (compared to Col-0). This ensured that regions enclosing single nucleotide polymorphisms (SNPs) were not picked as guide sequences. Lastly, cloning sequences were added at the 5' end of the 20nt oligos: 5'–ATTG–20nt guide sequence–3' and 5'–AAAC–20nt guide reverse complement sequence–3' (*Table 1*).

Targeted exon	Name oligo (20 nt)	Primer orientation	Sequence 5' – 3'
Exon 1	Pnsl1_E1_1F	Forward	ATTGACCACAGCGGATTGAGAGTG
Exon 1	Pnsl1_E1_1R	Reverse	AAACCACTCTCAATCCGCTGTGGT
Exon 1	Pnsl1_E1_2F	Forward	ATTGTTGGTGAGAAACCACCACAG
Exon 1	Pnsl1_E1_2R	Reverse	AAACCTGTGGTGGTTTCTCACCAA
Exon 2	Pnsl1_E2_1F	Forward	ATTGAAACAACAAGCTTTGAGTGA
Exon 2	Pnsl1_E2_1R	Reverse	AAACTCACTCAAAGCTTGTTGTTT
Exon 2	Pnsl1_E2_2F	Forward	ATTGCAAGCTTTGAGTGATGGATT
Exon 2	Pnsl1_E2_2R	Reverse	AAACAATCCATCACTCAAAGCTTG

***Table 1* | Guide RNA sequences for *PnsL1* (AT2G39470) CRISPR/Cas9 (spCas9) Knock-Out constructs**. Forward guide sequences correspond to 20nt oligos located in the non-coding DNA strand, downstream to the PAM site (NGG). Reverse complement guide sequences pertain to the coding strand. Nucleotides highlighted in yellow correspond to manually added cloning sequences that do not belong to the targeted oligonucleotide. These are required to insert the hybridized oligos in level 1 shuttle vector.

Forward and reverse sequences were diluted in MiliQ water and mixed at 10 µM, denatured at 98°C for 5 min and hybridized by cooling down at room temperature. Annealed oligos consisted of the complementary 20nt guide RNA sequences with the cloning primers flanking at 5'- ends as single stranded overhangs. 1:200 dilutions (50 fmol/µl) were prepared to proceed with cloning.

First, sgRNA transcriptional units (TU) were assembled by cloning the designed guide RNA sequences in "sgRNA shuttle vectors" (*Figure 4*)[66,67]. Three different shuttle vectors were employed: M1E (pDGE331), M1 (pDGE332) and M2E (pDGE334). These contain specific overhangs for posterior cloning steps into the "recipient/transformation vector" as a single sgRNA TU (M1E, to clone into recipient vector directly) or as two consecutive sgRNA TUs (M1 and M2E, with overlapping overhangs). Different oligo combinations were planned, and guide RNA sequences were cloned into the shuttle vectors accordingly.

The restriction/ligation was performed in a total volume of 10 µL containing 20 fmol (≈ 60 ng) of the shuttle module, 50 fmol of hybridized oligos, *BpiI* (0.3 u/µl), BSA (0.1 µg/µl), T4 DNA Ligase (0.03 u/µl) and T4 DNA 1x ligation buffer, diluted in Milli-Q water. The restriction/ligation reaction was carried out

in 30 cycles of 37 °C for 2 min – 16 °C for 5 min, followed by enzyme inactivation steps at 50°C for 10 min and 80 °C for 10 min.

5 µl of the ligation product (≈ 30 ng) were used to transform 50 µl of Mach1 *Escherichia coli* competent cells by heat shock method[68]. Positive selection of monoclonal transformant colonies was done on LB-Agar plates containing 100 µg/mL carbenicillin (Carb). Single colonies were inoculated in Liquid LB-Carb selective media (3 mL) and grown over night (16 h). Recombinant plasmid DNA was extracted by Miniprep alkaline lysis method[69].

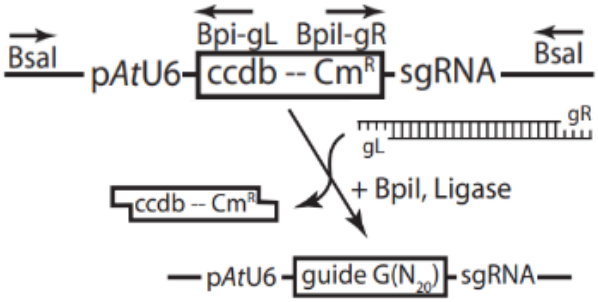

***Figure 4* | Generation of single guide RNA transcriptional unit (sgRNA TU) via shuttle vector**. Overall vector architecture consists of an A. thaliana U6 promoter (pAtU6), a ccdB negative selection cassette (with chloramphenicol resistance *Cm^R^* and *ccdB* toxin genes), and a tracRNA sequence (denoted as sgRNA). It also carries the carbenicillin resistance *Carb^R^* gene for positive selection. The ccdB cassette contains a *Bpi*I enzyme restriction site that enables introduction of the two hybridized oligonucleotides in a single restriction/ligation step. The designed guide RNA then ligates to pAtU6 and the tracRNA (scaffold for the Cas9 nuclease), thereby forming the sgRNA TU. The resulting ligation is flanked by *Bsa*I recognition sequences for posterior cloning into the "transformation vector" via Golden Gate Assembly. Figure from [66].

Recombinant level 1 constructs were then utilised to introduce the sgRNA TU into the level 2 transformation vector (pDGE347) (*Figure 5*)[66,67]. Different cloning reactions were conducted to generate a range of transformation modules with variable sgRNA TU combinations: 1sgRNA constructs with a single sgRNA TU and 2sgRNA constructs coupling two sgRNA TU, belonging to the first and/or second exon. The restriction/ligation solution was composed of 20 fmol (≈ 300 ng) of the recipient vector, 20 fmol (≈ 40 ng) of sgRNA TU shuttle module, *BsaI* (1 u/µl), BSA (0.1 µg/µl), T4 DNA ligase (0.25 u/µl) and T4 DNA 1x ligation buffer, diluted up to 20 µl with Mili-Q water. The reaction steps were followed described above but increasing the number of 37 °C – 16 °C cycles to 50.

Once again transformation of 50 µl Mach1 *E. coli* competent cells was done by heat shock supplying 5 µl (≈ 75 ng) of the resulting ligation. Transformant monoclonal colonies were selected in LB-Agar plates and transferred to liquid selective LB media, both containing 50 µg/mL spectinomycin. Stocks of all bacterial liquid cultures were prepared by mixing with glycerol 50% (50/50). Recombinant transformation plasmids were isolated by Miniprep. Finally, a restriction digestion was done with *Pst*I to test whether the plasmids had the expected sizes.

***Figure 5* | pdGE347 recipient or transformation vector.** Contains the FAST (fluorescence-accumulating seed technology) marker for identification of transformed seeds, the *Bar* gene conferring resistance to bialaphos (bar) herbicide and the zCas^i^ sequence for Cas9 endonuclease expression under control of the *Arabidopsis thaliana* RP5a promoter (pRPS5a). The ccdB negative selection cassette carrying the *ccdB* toxin and the chloramphenicol *Cm^R^* resistance is flanked by *Bsa*I restriction sites for substitution with the sgRNA TU. *Spec^R^* gene is also included for spectinomycin resistant positive selection. LB: Left Border (5'), RB: Right Border (3'). Figure from [66].

2.5 Phenotyping

Phenotyping assays were conducted in the "Robin" PSI PlantScreen™ system, automated platform that enables simultaneous screening of up to 20 *Arabidopsis* plants.

One major phenotyping experiment was carried out to assess photosynthetic performance of the different genotypes. 180 plants of both Bur and Col background genotypes were included. These were separated in two light treatment groups, 60 plants "Constant light" (n = 6 Bur and n =5 Col) and 120 plants "Fluctuating light" (n = 12 Bur and n = 11 Col). Growth conditions were kept constant for both groups during the first 19 days at 200 µmol photons m^{-2} s^{-1} in 12h light/darkness cycle. The last 5 days the "Fluctuating light" group received a light treatment based on the 3rd day of the DEPI system from Michigan State University (*Suplementary Figure 1*)[44]. This consisted of days with "sinusoidal" illumination that was raised every 30 minutes with 8-minute periods with doubled light intensity, so that the peak was 1000 µmol photons m^{-2} s^{-1}. Plants were then phenotyped in the Robin 24 days after sowing.

A schematic representation of the phenotyping protocol can be found in *Figure 6*. This was employed to infer photosynthetic parameters based on the pulse amplitude modulation (PAM) of chlorophyll fluorescence yield technique[70]. Phenotyping started at 8am when plants were in the last hour of their night period. This allowed direct assessment of four 4 x 5 randomized blocks (x1 "Constant", x3 "Fluctuating") without prior dark adaptation. The rest of the plants were dark-adapted during 30 minutes in an opaque box before measurements. Once introduced in the Robin, plants were further dark adapted for 10 minutes. The fluorescence in the darkness was determined (F_o). This was followed by a saturating light pulse (SP) applied to block all PSII reaction centres, obtaining the maximum peak of chlorophyll fluorescence (F_m).

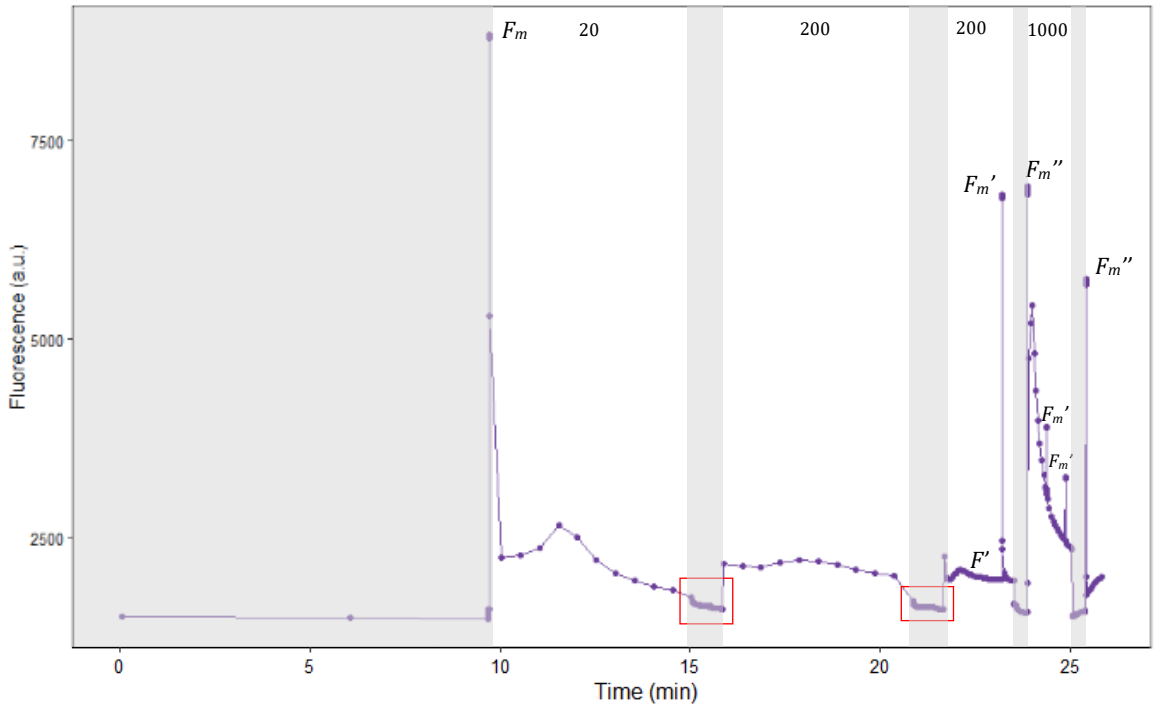

***Figure 6* | Phenotyping protocol for CEF & NPQ monitoring.** First, 10 minutes of adaptation in darkness (grey shaded areas) with a saturating light pulse at the end (*F_m*). Subsequently the post-illumination fluorescence increase is measured after 20 µmol m^{-2} s^{-1} and 200 µmol m^{-2} s^{-1} periods, when turning off actinic light (red marked areas, depicted in *Figure 5*). Actinic light is then turned on (*F'*) and another pulse is applied (*Fm'*). Light is turned off later and far-red light is supplied. Finally, an additional saturating pulse is given (*Fm''*) and actinic light is turned on at 1000 µmol m^{-2} s^{-1}. The last step from darkness to saturating pulse is repeated. Numbers on top of the plot sections indicate light intensity in µmol m^{-2} s^{-1} . Dots correspond to points where absolute fluorescence was measured. Y axis corresponds to raw fluorescence values (arbitrary units, a.u.), X axis depicts duration time (minutes). Protocol designed by Tom Theuween.

Actinic light (AL) – here also referred to as low light (LL) – was turned on next in two periods of 5 minutes at 20 and 200 µmol photons m^{-2} s^{-1}, each with 50 seconds of darkness added at the end. NDH activity was measured after every period as described in[71], by monitoring the post-illumination fluorescence raise (PIFR) in the dark (*Figure 7*). Chlorophyll fluorescence was quantified right after turning AL off, taking the minimum value recorded during the first 12 seconds (F_o'), and the maximum at the peak of the fluorescence increase (F_p), between 24 and 36 seconds after darkness. The fluorescence difference ($F_p - F_o'$) was normalised against the F_m value (*Equation 3*).

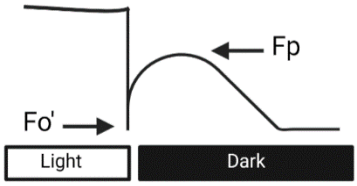

$$NDH = \frac{(F_P - F_o')}{F_m} \qquad \textit{(Equation 3)}$$

Figure 7 | Schematic model of transient fluorescence increase after turning off actinic light. Increase in fluorescence is caused by the recycling of electrons throughout the chain, attributed to NDH supercomplex activity.

AL was turned on at 200 µmol photons m^{-2} s^{-1} for other 2 minutes, and the steady chlorophyll fluorescence state was measured (F'), indicator of the stable photosynthetic rate. Via application of another SP, maximum fluorescence during AL illumination was obtained (F_m'). Active photosynthetic rate was calculated then, by measuring Φ_{PSII} in the light (*Equation 4)*[33,72].

$$\phi_{PSII} = \frac{(F_m' - F')}{F_m'} \qquad \textit{(Equation 4)}$$

NPQ values were then acquired by determining the reduction in fluorescence between F_m and F_m', which corresponds to the non-photochemically quenched energy (*Equation 5*)[33,72]:

$$NPQ = \frac{F_m - F_m'}{F_m'} = \frac{F_m}{F_m'} - 1 \qquad \textit{(Equation 5)}$$

Next AL was turned off and far-red (FR) light was activated for 20 seconds, in order to achieve relaxation of the fast components of NPQ. By supplying an additional SP (F_m'') short- and long-term recoveries were estimated as indicators of qE and qI, respectively (*Equations 6 & 7*)[73].

$$qE = \frac{F_m}{F_m'} - \frac{F_m}{F_m''} \qquad qI = \frac{(F_m' - F_m'')}{F_m''} \qquad \textit{(Equation 6 \& 7)}$$

Finally, high intensity light was supplied at 1000 µmol photons m^{-2} s^{-1} for 1 minute. F' and F_m' were obtained in the same manner so as to measure all parameters again under high light (HL).

In the produced dataset values corresponding to dead plants were manually removed. Data analysis was carried out for light treatment per separate, focusing on exploring the genetic variability. A mixed model was designed to get BLUES for genotype effects, including the blocks as random effects (*Equation 8*). A second model was also applied to study the plasmotype and copy.nr effect as well as their interaction (*Equation 9*). REML method was applied to calculate variance components with the lme4 package. Estimated marginal means computed with the emmeans package were utilised to evaluate contrasts among genotypes.

$$\underline{Y} = Genotype + \underline{Block} + \underline{\varepsilon} \qquad \textit{(Equation 8)}$$

$$\underline{Y} = Copy\ nr. + Plasmotype + Copy\ nr. \times Plasmotype + \underline{Block} + \underline{\varepsilon} \qquad \textit{(Equation 9)}$$

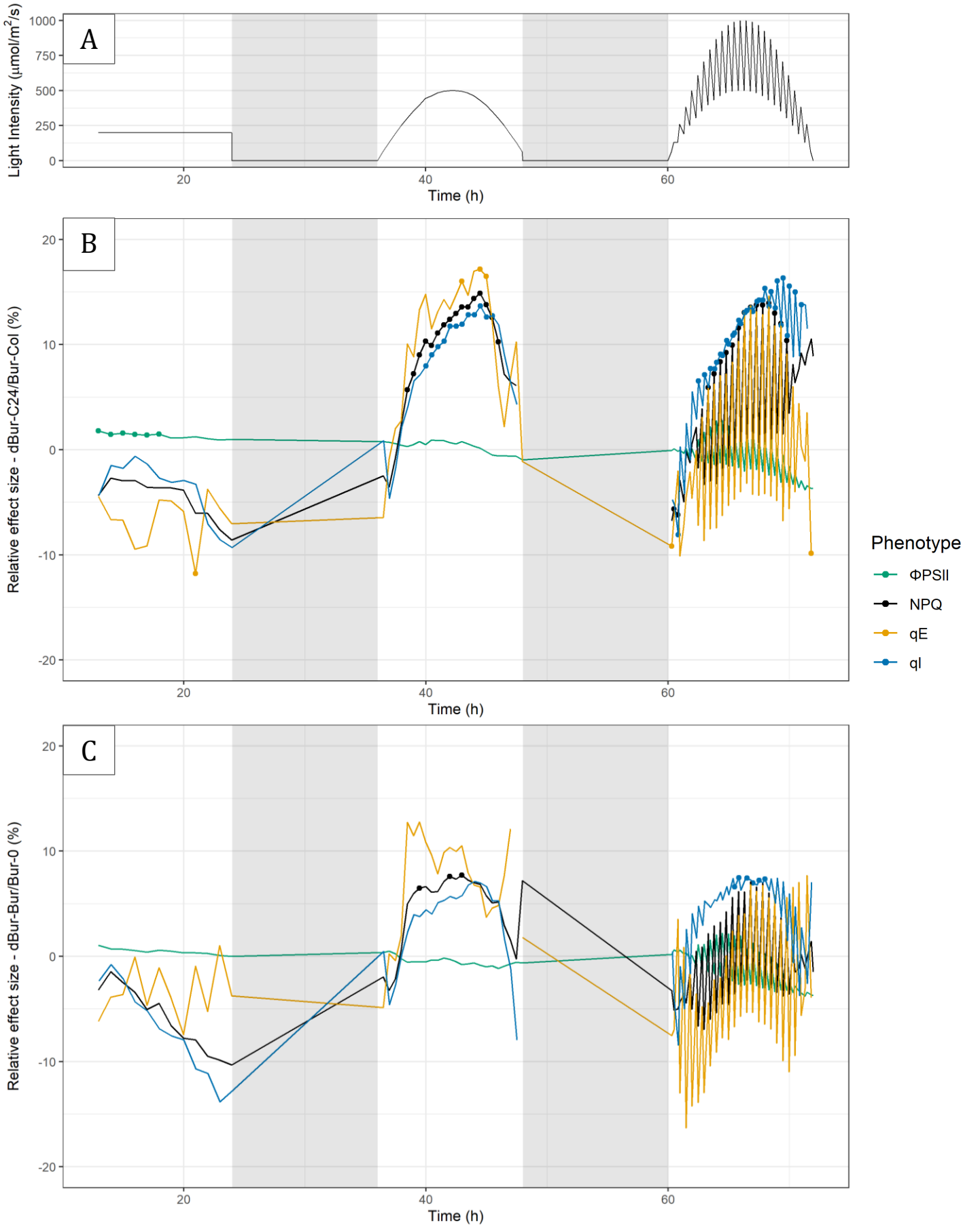
A
Light Intensity (µmol/m²/s)
1000
750
500
250
0
20
40
60
Time (h)
B
Relative effect size - dBur-C24/Bur-Col (%)
20
10
0
-10
-20
20
40
60
Time (h)
Phenotype
ΦPSII
NPQ
qE
qI
C
Relative effect size - dBur-Bur/Bur-0 (%)
20
10
0
-10
-20
20
40
60
Time (h)

Figure 8 | **Relative effect sizes of the nuclear locus duplication in photosynthetic performance**. Four photosynthetic phenotypes are depicted: Efficiency of phosystem II (Φ_{PSII}, green), overall non-photochemical quenching (NPQ, black), fast-response NPQ (qE, yellow) and photoinhibition slow NPQ (qI, blue) **A)** DEPI light system from Michigan State University. Three consecutive days are shown, with constant (day 1), sinusoidal (day 2) and fluctuating light intensity (day 3), starting at 12 h. The black line indicates the light intensity under which all of the parameter values were measured. Nights are represented by grey shaded areas. **B)** Relative effect size of the nuclear locus duplication estimated by comparing $dBur^{C24}$ vs. Bur^{Col} calculated as ($dBur^{C24}/Bur^{Col}$ – 1) *100. **C)** Relative effect size of the nuclear locus duplication estimated by comparing $dBur^{Bur}$ vs. Bur-0 calculated as ($dBur^{Bur}$/Bur-0 – 1) *100. Dots on the lines represent time points where significant differences were found between genotypes ($p < 0.05$).

3.1 NPQ phenotype in dBur is affected by nuclear locus duplication and the plasmotype

As a first step in the analysis, the unpublished DEPI data involving the dBur cybrids was analysed with an emphasis on the duplication. To evaluate its impact on photosynthetic performance, examination of the phenotype concentrated on Φ_{PSII}, NPQ, qE and qI parameters. Φ_{PSII} was employed as a proxy for total photosynthetic efficiency, which is negatively affected by increases in NPQ. To investigate NPQ, besides focusing in total NPQ, qE was also studied as the principal NPQ component, while qI was employed as indicator of photoinhibition under the received light. The duplication relative effect size was estimated by comparing $dBur^{Bur}$ to Bur-0 and $dBur^{C24}$ against Bur^{Col} (based on the assumption that C24 and Col plasmotypes are not different[41]). *Figure 8* displays the developement of the Φ_{PSII}, NPQ, qE, and qI parameters as a function of time and lighting conditions (constant "flat", sinusoidal and fluctuating light, *Figure 8* A). The analysis revealed that the duplication effect in was largest at the peak of the sinusoidal day (500 µmol photons m^{-2} s^{-1}), and that was hardly decreasing in the fluctuating light. Right at the middle of the sinusoidal day (44 h) $dBur^{C24}$ had up to 17% higher qE ($p = 0.03$) and ~ 15% more NPQ than Bur^{Col} ($p < 0.001$) (*Figure 8* B). $dBur^{Bur}$ on the other hand, only exhibited a relative increase in NPQ of 7-8% ($p \leq 0.03$) that was significant (*Figure 8* C). This observation suggested that the phenotype was less pronounced in combination with the Bur plasmotype present, implying the possible occurrence of a plasmotypic effect that initially was not considered. As a result, the subsequent analysis concentrated on the plasmotype and nucleotype impacts on NPQ, as well as their interaction.

The study of the DEPI data focusing on copy number and plasmotype indeed revealed the occurrence of divergent effects in NPQ. In *Figure 9*, relative effect sizes of copy number and plasmotype are estimated as "double" vs. "single" and C24 vs. Bur. During the first day of the DEPI treatment, the C24 plasmotype exhibits significantly higher qE when compared to the Bur plasmotype (*Figure 9* B). In constant light conditions, the relative effect difference in qE is about 6 to 14% during most of the day (16 -24h, $p \leq 0.02$). At the beginning of the sinusoidal day, the C24 plasmotype presents 6.5% higher qE than Bur, when light is about 200 µmol photons m^{-2} s^{-1} (*Figure 9 B*). The increase in light intensity however diminishes the differences in plasmotypic effects. It is not until the light returns to 200 – 250 µmol photons m^{-2} s^{-1} that the relative effect size becomes visible again (*Figure 9* B). The opposite occurs with NPQ and qI, where the C24 plasmotype shows to have a 4 to 5% lower effect than Bur as light intensity increases ($p \leq 0.05$) (*Figure 9 B*). Lastly, the light fluctuations on the third day show that the plasmotypic relative effect sizes in qE resemble the ones observed on the sinusoidal day. During the first two hours, qE is significantly higher in C24 than Bur, approximating 13% difference when light is 250 µmol photons m^{-2} s^{-1} (*Figure 9* B). Once again, when light intensity increases distinctive plasmotypic effects disappear, but when returning to lower intensities at the end of the fluctuations, qE returns to be higher in C24 when contrasted to Bur, reaching maximum difference of 16% at 70h ($p = 0.0003$) (*Figure 9* B). Similarly, total NPQ in the C24 plasmotype appears to be considerably higher than the Bur only at the end of the day, by 7% (72h, $p = 0.03$). qI, on the other hand, is lower in the C24 than the Bur plasmotype at the start of the oscillations (4 % at 62h, $p = 0.017$). Φ_{PSII} appears to be mostly unaffected by the different plasmotypes throughout the whole DEPI treatment (*Figure 9* B).

When looking at copy number (*Figure 9* C), it is noticeable that the relative effect size of the duplication under constant-day conditions is to lower NPQ rather than increase it. Overall NPQ is relatively reduced in dBur throughout the 12 hours of the first day, with the difference being the greatest towards the end (23.96h), with a 9% drop (pairwise comparisons 1 copy.nr – 2 copy.nr, $p = 0.02$). qI follows a similar

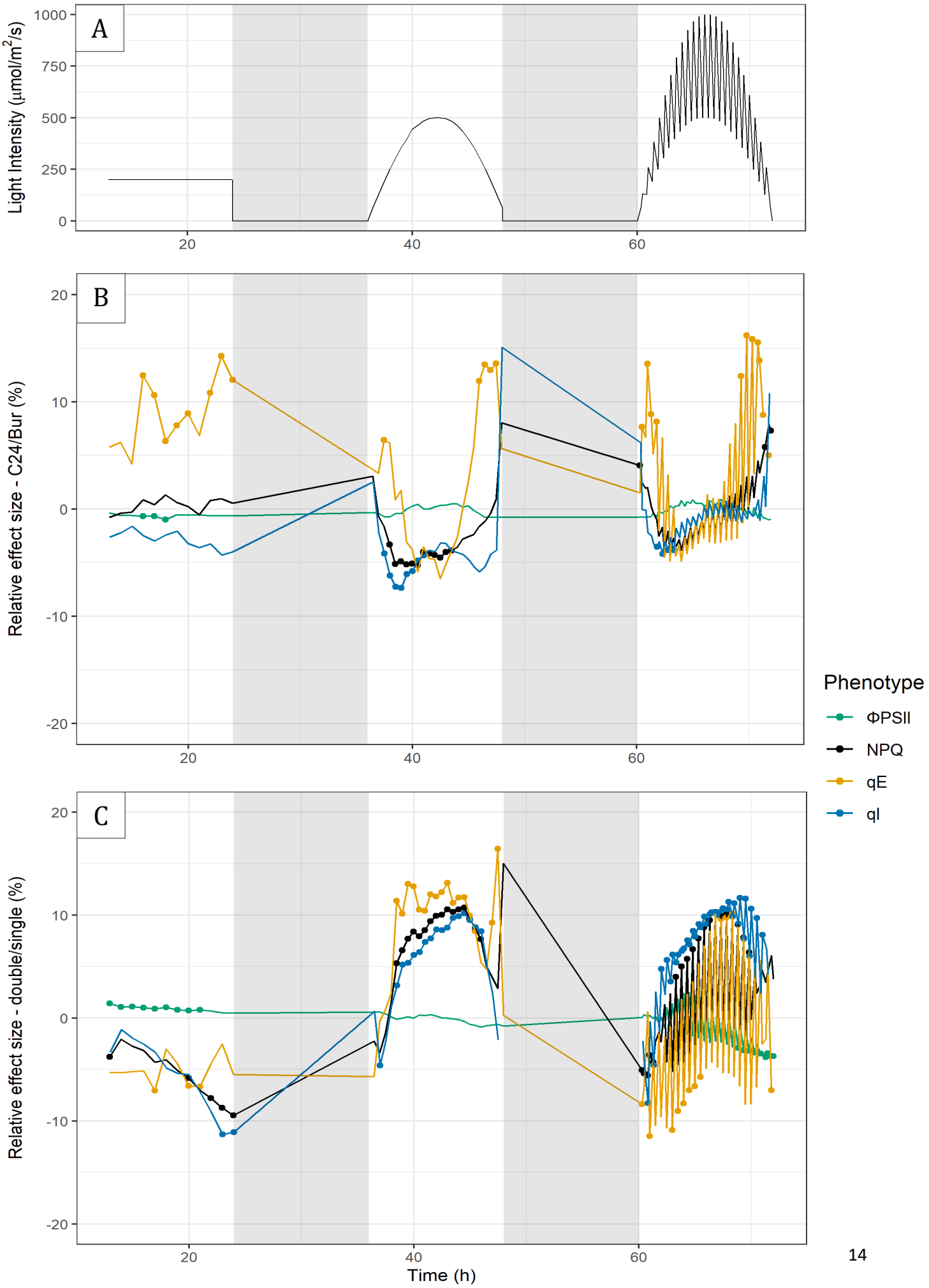
A
Light Intensity (µmol/m²/s)
1000
750
500
250
0
20
40
60
B
Relative effect size - C24/Bur (%)
20
10
0
-10
-20
20
40
60
C
Relative effect size - double/single (%)
20
10
0
-10
-20
20
40
60
Time (h)
Phenotype
ΦPSII
NPQ
qE
qI

***Figure 9* | Relative effect sizes of the nuclear locus duplication and the plasmotype in photosynthetic performance**. Four photosynthetic phenotypes are depicted: Efficiency of phosystem II (Φ_{PSII}, green), overall non-photochemical quenching (NPQ, black), fast-response NPQ (qE, yellow) and photoinhibition slow NPQ (qI, blue) **A)** DEPI light system from Michigan State University. Three consecutive days are shown, with constant (day 1), sinusoidal (day 2) and fluctuating light intensity (day 3), starting at 12 h. The black line indicates the light intensity under which all of the parameter values were measured. Nights are represented by grey shaded areas. **B)** Relative effect size of the C24 plasmotype compared against the Bur plasmotype, calculated as (C24/Bur - 1) *100. **C)** Relative effect size of the nuclear locus duplication over the single copy of the locus, estimated as (double/single - 1) *100. Dots on the lines represent time points where significant differences were found between plasmotypes or locus copy number ($p < 0.05$).

trend, with the highest decline in dBur (11 %) near the end of the day (22.99 h) ($p = 0.029$). qE is more stable throughout the day, hovering around a negative impact size of 5%, with only three significant dips of 6-7% ($p = 0.04$) at 17, 20, and 21h. Relative drops in NPQ in dBur do not appear to have a significant influence on Φ_{PSII} though, which is 1% higher during the first half of the day (12 – 18h) ($p < 0.01$) (*Figure 9* C). Nonetheless, when settings are altered on the second day and sinusoidal light is provided, the locus duplication effect in NPQ turns positive when compared to sBur (*Figure 9* C). All NPQ parameters are higher in dBur than sBur as light intensity rises, peaking around the middle of the day and decaying towards the end. Overall NPQ and qI in dBur peak at maximum light intensity by 10% (500 µmol photons m^{-2} s^{-1}, 44 h) ($p \leq 0.001$), whereas maximum duplication effects in qE are detected at 13% (43 h) ($p = 0.003$). No meaningful effects are detected for Φ_{PSII} (*Figure 9* C).

When lights are fluctuated on the third day, the high variability caused by the duplication becomes evident. *Figure 10* displays a zoom in of the last 12 h of the DEPI treatment. It is worth noting that NPQ and qE exhibit a similar trend: the biggest effects of the duplication are visible at the low light (LL) conditions after a HL period (*Figure 10* B). Maximum effect sizes in dBur when compared to sBur are detected close to the middle of the fluctuating day (66-68 h). In transitions from 8-minute HL to 20-minute LL intervals, duplication relative effect size in NPQ and qE shifts from being not significantly different at HL (1000 µmol photons m^{-2} s^{-1}), to increasing to up to 10% when lights are lowered (500 µmol photons m^{-2} s^{-1}) (NPQ $p = 0.000$, qE $p < 0.05$) (*Figure 10* B). The duplication also exhibits a distinguishable effect in the qE phenotype when compared to the single copy. During the first half of the day, light raises after LL periods reveal that the relative effect in qE is negative. This is minimum at -11% at 61 h ($p = 0.009$) and 63 h ($p = 0.01$), when

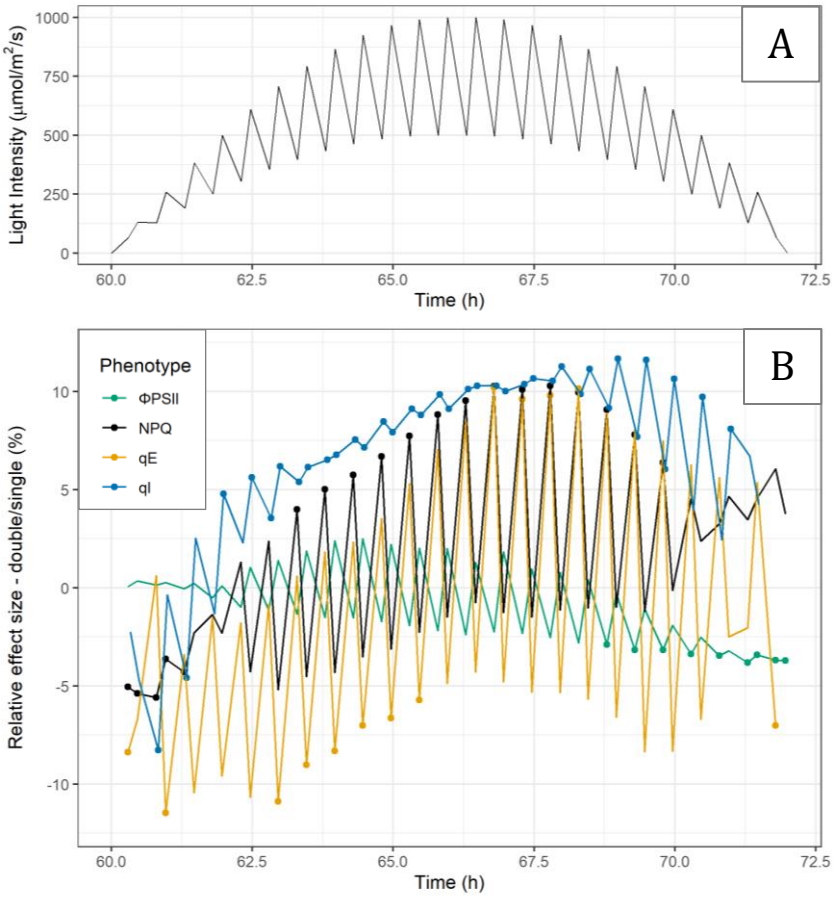

***Figure 10* | Relative effect sizes of the nuclear locus duplication in photosynthetic performance**. Four photosynthetic phenotypes are depicted: Efficiency of phosystem II (Φ_{PSII}, green), overall non-photochemical quenching (NPQ, black), fast-response NPQ (qE, yellow) and photoinhibition slow NPQ (qI, blue) **A)** 3rd day of the DEPI light treatment from Michigan State University, where fluctuating light is applied, starting at 60 h. The black line indicates the lighting conditions under which all of the parameter values were obtained. **B)** Relative effect size of the nuclear locus duplication over the single copy of the locus, estimated as (double/single - 1) *100. Dots over the lines represent time points where significant differences were found between copy number ($p < 0.05$).

light intensity is 250 and 700 µmol photons m^{-2} s^{-1}, respectively. Nevertheless, the negative effect persists until HL reaches almost 1000 µmol photons m^{-2} s^{-1}, being -6% (p = 0.025) (*Figure 10* B). The extent of the duplication effect tends to be more consistent for qI, which grows throughout the day without being as impacted by oscillations. The effect magnitude is larger after HL periods in this instance, with a maximal impact of 11% at 68 h (p = 0.000) (*Figure 10* B). In this situation when comparing dBur to sBur, Φ_{PSII} does show to be affected by the variable light or changes in NPQ, as dBur presents 3-4% lower efficiency near the end of the day (69-72 h, $p < 0.05$) (*Figure 10* B).

To summarise, it was discovered that the influence of the duplication on the dBur photosynthetic phenotype was highly variable and very dependent on the light environment (*Figure 9* C, *Figure 10* B). Similarly, the effects of the plasmotype on the phenotype showed to be strongly reliant on the light conditions (*Figure 9* B). Finally, both plasmotype and duplication exhibited diverging effects – particularly in qE – that arise in a light-intensity dependent transitional pattern (*Figure 9* B & C). No significant interactions between copy number and plasmotype were detected for any of the parameters, with the exception of the last 3 hours of the fluctuating light day, when the interaction was discovered to be significant for qI ($p < 0.05$).

3.2 *PnsL1* expression is higher in dBur and not regulated by increase in light intensity

Based on the DEPI data analysis results, it was postulated that the major shift in NPQ response due to the duplication at the peak of the sinusoidal day (*Figure 9* C, 500 µmol photons m^{-2} s^{-1}) could be caused by a change in gene expression involving *PnsL1*. To test this hypothesis, quantification of *PnsL1* mRNA levels in Bur cybrids and Bur-WT was conducted in plants before (constant light) and after sinusoidal light treatment.

RT-qPCR assays confirmed that the *PnsL1* expression was indeed higher in the dBur cybrids due to the locus duplication (*Figure 11*). Both under constant (*Figure 11* A) and sinusoidal light conditions (*Figure 11* B), $dBur^{Bur}$ and $dBur^{C24}$ proved to have doubled transcription of the gene when compared to Bur-WT. Additionally, it was also confirmed that the sBur cybrids did have expected single copy of the locus as they did not differ significantly from-WT.

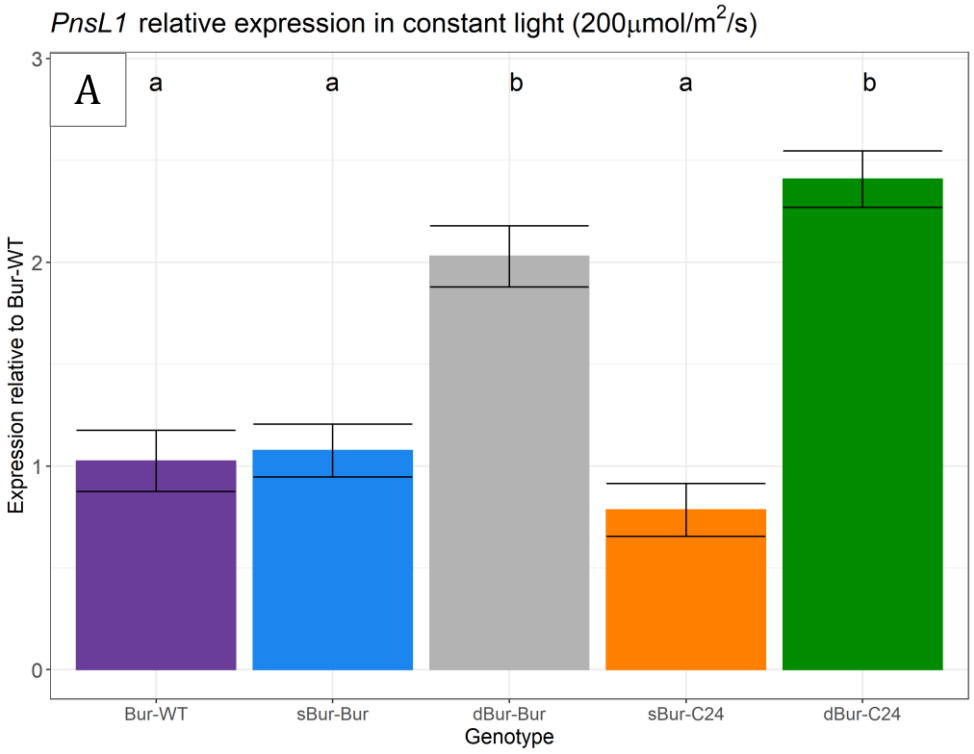

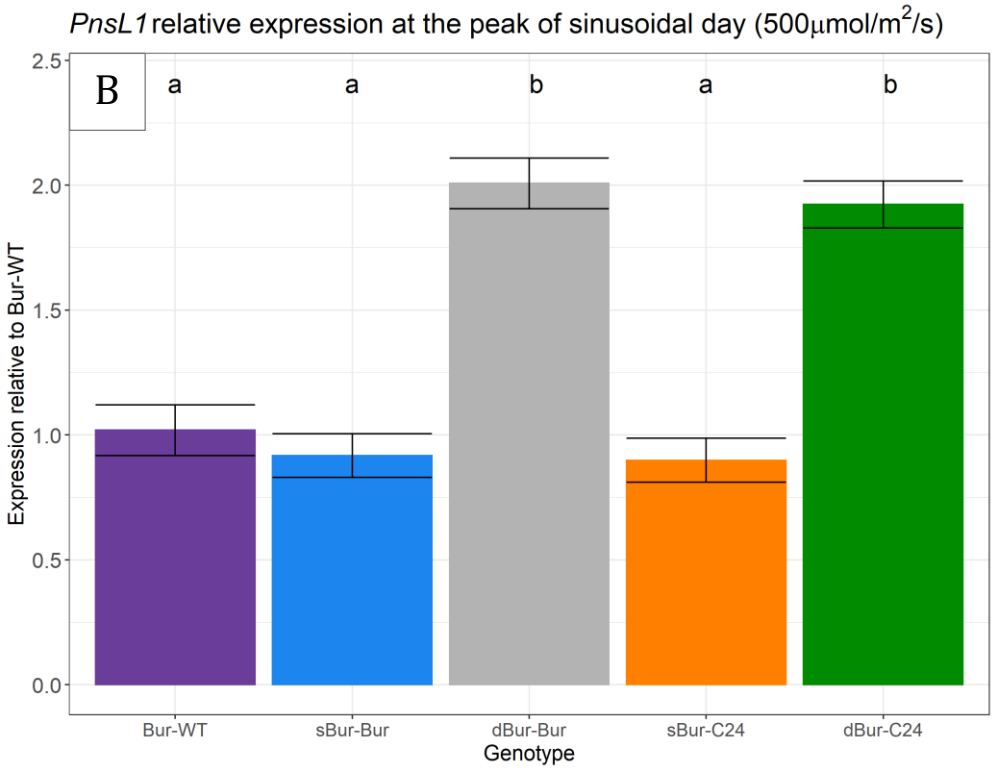

***Figure 11* | *PnsL1* expression in Bur cybdrids relative to Bur-WT.** *Arabidopsis thaliana* Burren-0 wild-type (Bur-WT) and cybrids containing nuclear locus duplication ($dBur^{Bur}$ and $dBur^{C24}$) as well as a single copy of the locus ($sBur^{Bur}$ and $sBur^{C24}$), sampled before (constant light, **A**) and after (**B**) sinusoidal light treatment (n = 8). Cybrid genotypes in the X-axis are denoted as double/single nucleotype-plasmotype. Bars indicate geometric means of quantitative $2^{-\Delta Ct}$ values relativised against Bur-WT (=1) + standard error (SE). Different letters at the top of the bars represent statistically significant differences among genotypes (*p – value < 0.001*).

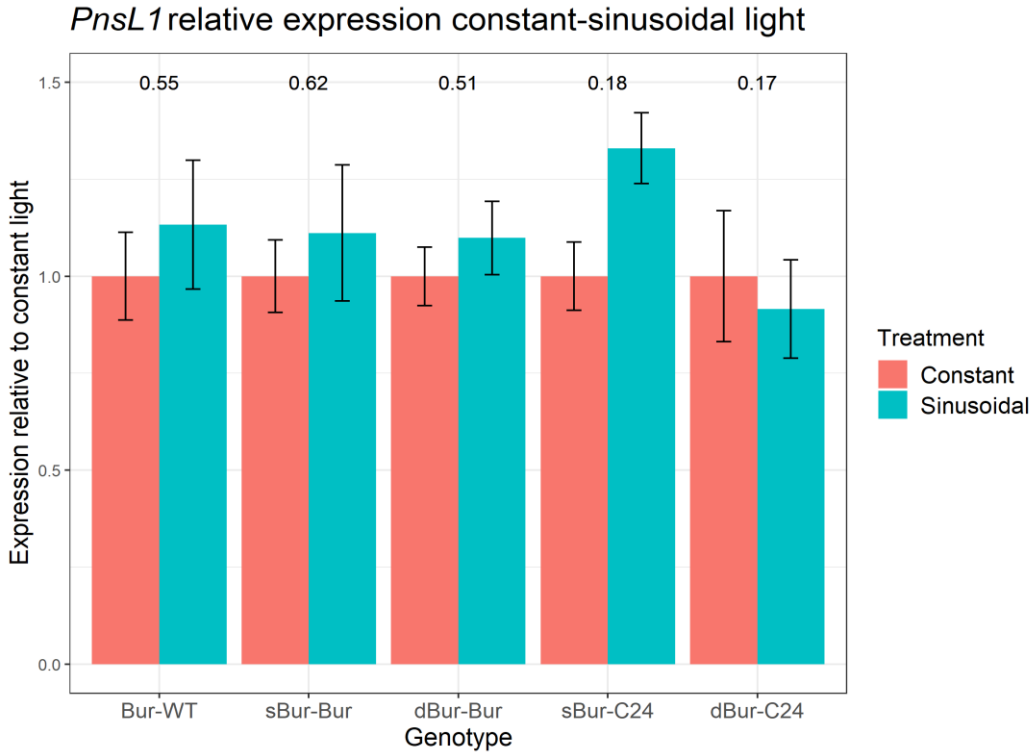

***Figure 12* | *PnsL1* expression change in Bur cybdrids and to Bur-WT under sinusoidal treatment, relative to constant light.** *Arabidopsis thaliana* Burren-0 wild-type (Bur-WT) and cybrids containing nuclear locus duplication ($dBur^{Bur}$ and $dBur^{C24}$) as well as a single copy of the locus ($sBur^{Bur}$ and $sBur^{C24}$), sampled before (constant light) and after sinusoidal light treatment (n = 8). Cybrid genotypes in the X-axis are denoted as double/single nucleotype-plasmotype. Bars indicate geometric means of quantitative $2^{-\Delta\Delta Ct}$ values calculated by relativising sinusoidal $2^{-\Delta Ct}$ to own $2^{-\Delta Ct}$ values prior treatment, constant light (=1), + standard error (SE). Numbers at the top of the bars represent *p-values* obtained by t-test for two sample comparison.

Relativisation of $2^{-\Delta Ct}$ before and after light treatment per genotype resulted in no significant differences in expression (*Figure 12*). In conclusion, it was demonstrated that expression of *PnsL1* does not increase when subjected to sinusoidal light increase and thus it is probably not regulated by shifts in light intensity.

3.3 Cloning of the CRISPR/Cas9 Knock-Out transformation vectors

So as to enable further investigation of potential implication of *PnsL1* duplication on the dBur photosynthetic phenotype, Golden Gate cloning of *PnsL1* gene in CRISPR/Cas9 KO constructs was attempted.

Starting with shuttle vector cloning, restriction and ligation reactions into shuttle vectors were successful, as well as the following *E. coli* transformation. However, plasmid extraction via bacterial lysis (Miniprep) yielded very low concentrations when measured with the Qubit fluorometer (Invitrogen), ranging from 3 to 30 ng/µL. The bacterial culture and lysis were repeated with comparable results. The acquired plasmid purifications did not include enough DNA material to assess if the constructs were the right size by running them in an agarose gel after enzymatic digestion (1000 µg needed). The amount of shuttle vector necessary to proceed with the cloning of the sgRNA into the transformation was not particularly large. Therefore, the restriction ligation reaction was attempted anyways. The transformation of bacteria with the reaction product resulted in the establishment of a few colonies on selection plates. When these were grown over night and plasmid extraction was performed, the technique produced low amounts in the same range as before. The digestion test (with *Pst*I) was tried on up to 10 µL of each DNA isolate, however when run in a gel, only the undigested positive control and the digested negative control could be detected.

To try again, a step back was taken, and the restriction ligation reaction into the transformation vector, as well as the subsequent stages, were carried out. However, the outcomes were consistent. Obtaining such low concentrations made it difficult to fulfil the sequencing company's standards (20 µL with 50 ng DNA/µL). At the end, *PnsL1* gene Golden Gate cloning procedure in CRISPR/Cas9 KO constructs did not result in the successful acquisition of the final transformation vector. Cloning activity had to be halted because the project's time frame had come to an end. Glycerol stocks were made from the last transformation's transformant colonies and preserved at - 80°C. Hopefully, they may be used to address the arose difficulties in the future.

3.4 Confirmation distinctive dBur photosynthetic phenotype in the Robin

To assess whether differences in dBur NPQ phenotype could be induced in the Robin, Φ_{PSII}, NPQ, qE and qI parameters were measured using two contrasting light intensities: Low light (LL, 200 µmol photons m^{-2} s^{-1}) or high light (HL, 1000 µmol photons m^{-2} s^{-1}). Measuring photosynthesis with the applied fluorescence methodology (*Figure 6*) revealed that dBur cybrids varied from the other genotypes (*Figure 13*, *Supplementary Figure 2*). The display of variation produced by genotype effects was significantly dependent not only in the measuring light, but also the received light treatment (constant or fluctuating light). Differential performance was especially visible in plants treated with fluctuating light (*Figure 13,* note that y axes differ per boxplot to highlight differences among genotypes). When measurements were done following the administration of 200 µmol photons m^{-2} s^{-1} (LL) in the Robin, it was discovered that dBur cybrids had greater qE than the sBur ($dBur^{Bur}$–$sBur^{Bur}$ and $sBur^{C24}$–$dBur^{C24}$ $p < 0.0001$), with $dBur^{C24}$ at the top ($dBur^{C24}$ – $dBur^{Bur}$ $p = 0.0016$) (*Figure 13* E). However, this did not appear to have an increasing effect in overall NPQ, since dBur cybrids showed to have lower NPQ values rather than greater ($p < 0.0001$) (*Figure 13* C). Photosynthetic efficiency was not affected when measured at LL in the Robin, this since there was no difference in Φ_{PSII} (*Figure 13* A). Furthermore, assessment of NPQ and qI showed that dBur cybrids not only had lower NPQ but also were less prone

to photoinhibition under LL ($p < 0.0001$) (*Figure 13* C & G). When NPQ was tested after the application of 1000 µmol photons m^{-2} s^{-1} (HL) in the Robin dBur cybrids not only exhibited lower qE values ($p \leq$

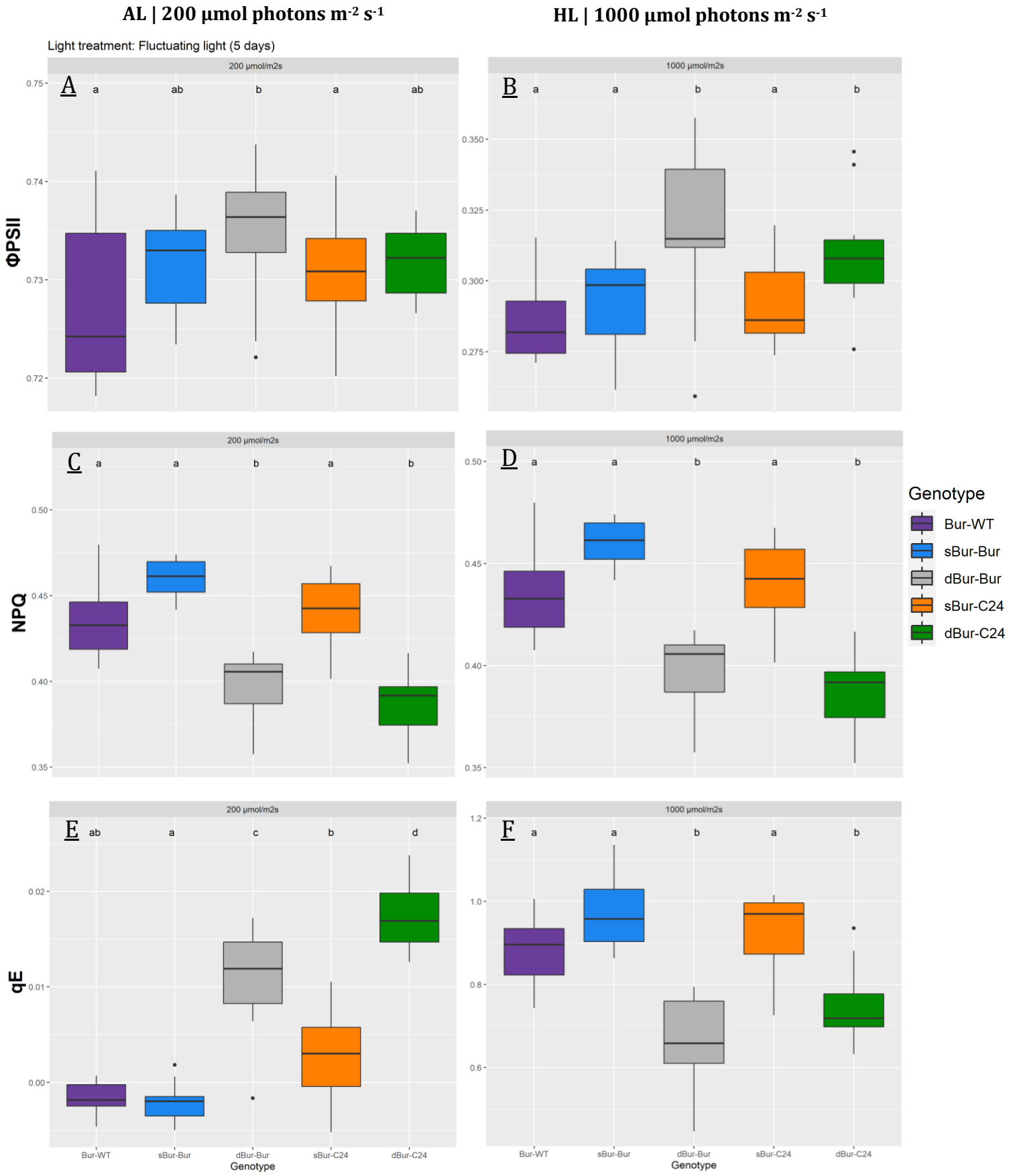

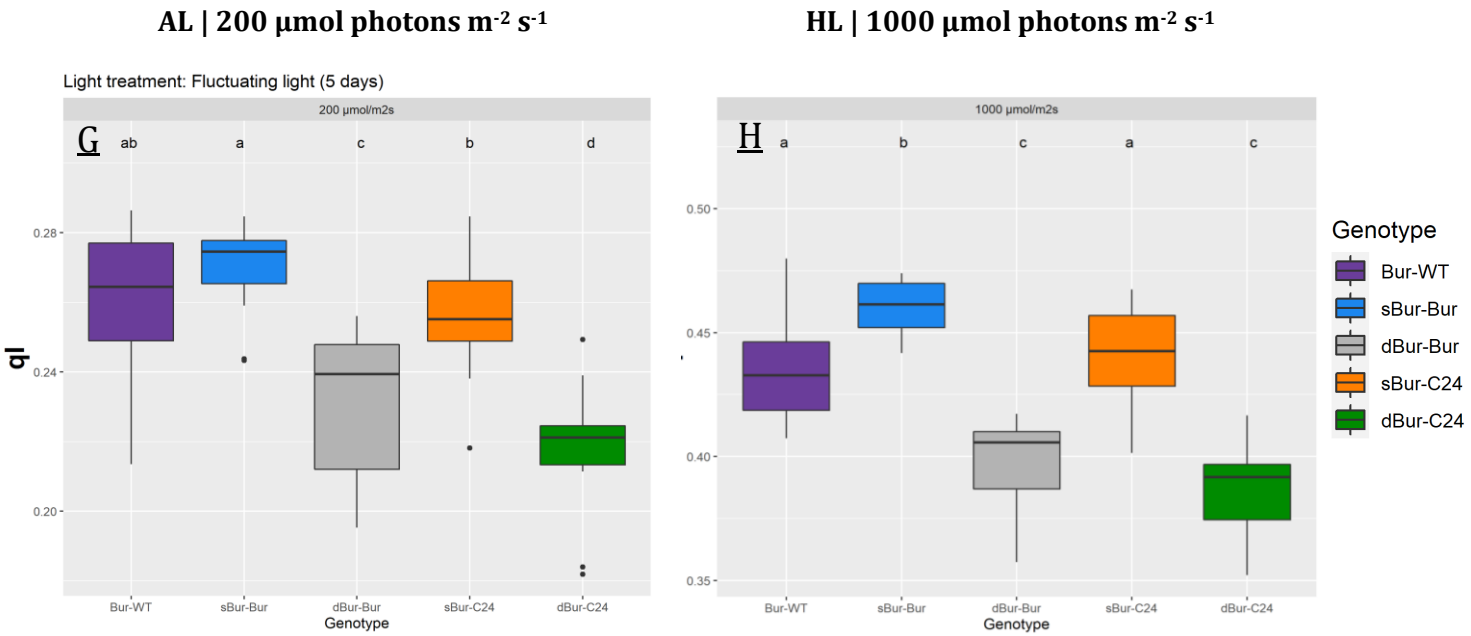

***Figure 13* | Photosynthetic performance of Bur-WT and Bur cybrids.** *Arabidopsis thaliana* Burren-0 wild-type (Bur-WT) and cybrids containing nuclear locus duplication ($dBur^{Bur}$ and $dBur^{C24}$) as well as a single copy of the locus ($sBur^{Bur}$ and $sBur^{C24}$), receiving fluctuating light treatment (n = 11). Cybrid genotypes in the legend are denoted as double/single nucleotype-plasmotype. Light intensity applied to infer photosynthetic parameters is displayed at the top of the plot columns, low light (LL, 200 µmol photons m^{-2} s^{-1}) and high light (HL, 1000 µmol photons m^{-2} s^{-1}). Φ_{PSII} refers to the efficiency of photosystem II under applied light conditions, measured as $(F_m'-F_p)/F_m'$. NPQ represents the photochemical quenching of light energy surplus activated as a protection mechanism against high light, estimated as $F_m/F_m' - 1$. qE is the fast NPQ component triggered by H^+ accumulation in the lumen, inferred as $(F_m/F_m') - (F_m /F_m'')$. qI represents the photoinhibitory NPQ occurring when Φ_{PSII} is damaged, calculated as $(F_m'- F_m'')/ F_m''$. See section 2.2 in Materials & Methods for further explication of the calculations. Boxes represent interquartile ranges with medians (black horizontal line) + spread of the data (whiskers). Note that scales in y axes differ per plot, as the focus is on emphasizing genetic differences rather than physiological. Different letters on top of the boxes represent statistically significant differences across genotypes in each individual boxplot ($p < 0.05$).

0.0002) (*Figure 13* F), but also lower NPQ ($p < 0.0001$) (*Figure 13* D). Correspondingly, the cybrids with the duplication proved to be more photosynthetically efficient under HL conditions, having higher Φ_{PSII} values than sBur plants (*Figure 13* B) ($sBur^{Bur}$–$dBur^{Bur}$ $p < 0.0001$, $sBur^{C24}$–$dBur^{C24}$ $p = 0.0069$). In line with this, dBur cybrids appeared to be less susceptible to photoinhibition ($p < 0.0001$) (*Figure 13* H). A similar pattern was detected in plants grown under constant conditions, however the differences among genotypes were not as significative (*Supplementary Figure 2*). Results of the constant light treatment resembled more the ones of the plants receiving fluctuation when parameters were assessed after application of HL. Only NPQ, qE and qI were found to differ significantly upon HL (*Supplementary Figure 2* D, F & H).

Lastly, analysis of the interactions between the duplication and the plasmotype in the data collected from plants receiving constant and fluctuating light treatment resulted in no significant outcome.

3.5 NDH mutants confirm efficacy of PIFR phenotyping protocol

The first step towards examination of phenotypic variation in NDH activity lied in ensuring the efficacy of the PIFR monitoring protocol in our experimental set up. As explained in section 2.2, PIFR was scrutinised in darkness after application of both 20 and 200 µmol photons m^{-2} s^{-1} (*Figure 6*). After 20 µmol photons m^{-2} s^{-1}, all genotypes in both constant and variable light treatments exhibited no increase in chlorophyll fluorescence, indicating that it was not a sufficient light intensity to phenotype NDH activity in our experimental settings. However, when measured after 200 µmol photons m^{-2} s^{-1}, the PIFR could be observed in all of the Bur cybrids, as well as Col-0 (*Figure 14* A). Furthermore, the fluorescence increase could be identified regardless of the received treatment, either fluctuating (*Figure 14*) light or constant light (*Supplementary Figure* 3). In line with prior research, PIFR was not detected in the *crr2-2*, *ndh01* and *pnsl1* Col mutants (*Figure 14* B). The absence of fluorescence increase in the NDH mutants demonstrated that measuring PIFR after 200 µmol photons m^{-2} s^{-1} in was a reliable method of evaluating NDH activity in the Robin. As a result, only NDH activity measured after 200 µmol photons m^{-2} s^{-1} was regarded in later assessment.

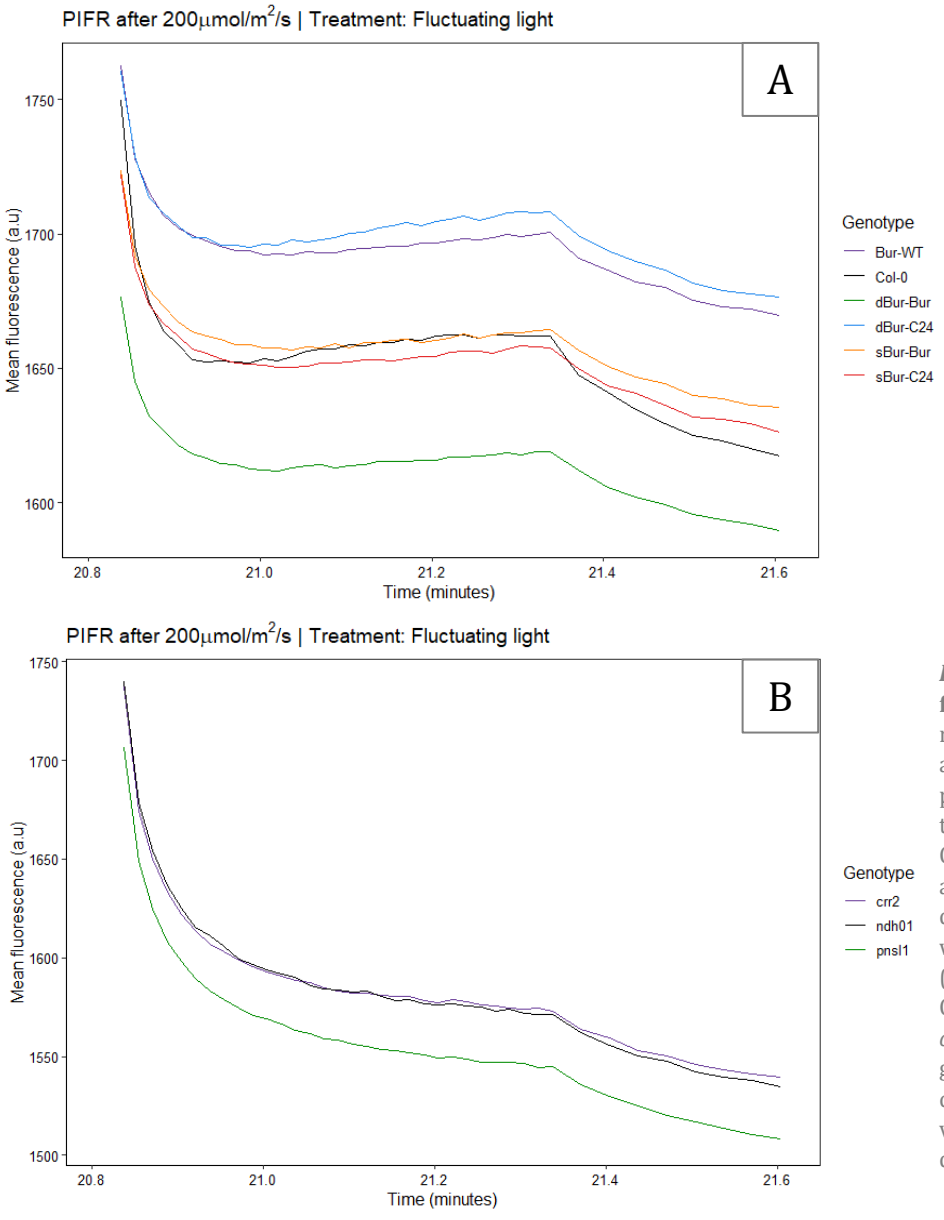

***Figure 14* | Post illumination fluorescence increase (PIFR)** monitored in the dark after application of 200 µmol m^{-2} s^{-1} in plants receiving fluctuating light treatment **A)** *Arabidopsis thaliana* Col-0 and Burren wild-type (Bur-WT) and cybrids containing nuclear locus duplication ($dBur^{Bur}$ and $dBur^{C24}$) as well as a single copy of the locus ($sBur^{Bur}$ and $sBur^{C24}$). **B)** *A. thaliana* Columbia NDH defective mutants *crr2*, *ndhO* and *pnsl1*. Lines represent genotypic fluorescence means. Y axis corresponds to raw fluorescence values (arbitrary units, a.u.). X axis depicts time (minutes).

3.6 NDH activity is affected by the duplication and the plasmotype

PIFR monitoring in the Bur genotypes revealed considerable genetic variations in NDH activity. These were discovered to be particularly reliant on the received light treatment, constant or fluctuating light (*Figure 15*).

When plants received constant light treatment, dBur^{C24} showed to be the genotype with the highest NDH activity (pairwise comparisons $p < 0.05$). sBur^{C24} also demonstrated to have increased NDH activity, which was lower than its counterpart (pairwise comparison dBur^{C24} – dBur^{Bur} $p = 0.0231$) but higher than the other cybrids. In terms of dBur^{Bur}, it was found that when exposed to constant light it was not considerably different from either sBur^{Bur} or Bur-WT (*Figure 15* Constant light).

Under fluctuating light conditions on the other hand, only dBur^{C24} was found to exhibit higher NDH activity when compared to the rest of the genotypes (pairwise comparisons $p < 0.001$). The remaining cybrids, including dBur^{Bur}, did not differ significantly from Bur- WT (*Figure 15* Fluctuating light).

Finding increased NDH activity in dBur^{C24} proved that nuclear locus duplication and NDH activity were correlated. On the other hand, the inability to detect any distinctive NDH activity in dBur^{Bur} under constant or fluctuating conditions, provided additional evidence of the existence of a plasmotypic effect determining the dBur photosynthetic phenotype. Analysis of the interaction between plasmotype and copy number effect revealed the existence of significant interactions under fluctuating light only (p = 0.006).

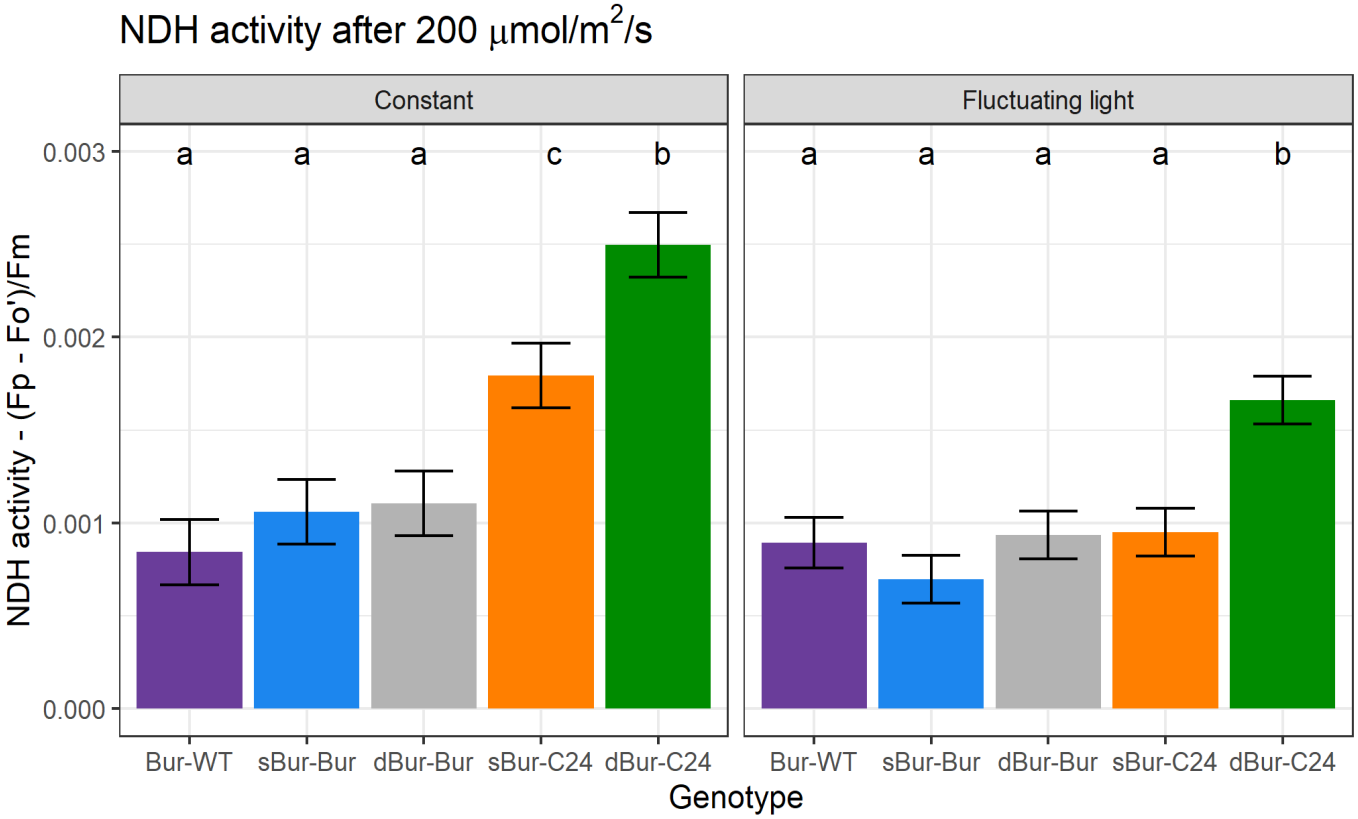

***Figure 15* | NDH activity in Bur-WT and Bur cybrids.** *Arabidopsis thaliana* Burren-0 wild-type (Bur-WT) and cybrids containing nuclear locus duplication (dBur^{Bur} and dBur^{C24}) as well as a single copy of the locus (sBur^{Bur} and sBur^{C24}) are shown. Cybrid genotypes in the X-axis are denoted as double/single nucleotype-plasmotype. Facet titles indicate received light treatment, constant (n = 6) and 5 days of light fluctuation (n = 11). NDH activity was quantified as described in[71] ($F_p - F_o' / F_m$ by monitoring the post illumination transient fluorescence increase in the darkness after application of 200 µmol photons m^{-2} s^{-1} actinic light (*Figure 7*). Bars represent arithmetic means + standard error (SE). Different letters at the top of the bars represent statistically significant differences among genotypes within treatments (*p – value < 0.05*).

4. DISCUSSION

4.1 Characterisation of the dBur NPQ photosynthetic phenotype

Characterising the NPQ and photosynthetic phenotype of dBur was the first purpose of this MSc thesis. To accomplish this goal, the original DEPI data that motivated this project was analysed.

Examination of the NPQ phenotype across three DEPI days with varied light settings revealed that the influence of the duplication in the dBur photosynthetic phenotype was more complicated than originally anticipated. Instead of finding constitutively increased NPQ as previously expected, the duplication showed to have a highly variable impact on the phenotype, which was very dependent on the light environment (*Figure 9* C). These results suggested that the consequences of the duplication would rather imply the adjustment of a more complex NPQ regulation mechanism. Moreover, it was discovered that the duplication was not the sole factor influencing the photosynthetic phenotype. The dBur phenotype showed to be dependent on the carried plasmotype as well, with the Bur plasmotype appearing to mitigate the impacts of the duplication when compared to C24 (*Figure 8* B & C). Similarly, the effects of the plasmotype on the phenotype showed to be strongly reliant on the light conditions (*Figure 9* B).

It was found that the duplication and plasmotype effects were not overlapping and that they arose in in a light-intensity dependent transitional pattern (*Figure 9* B & C). This trend could indicate that the duplication and plasmotype affect the phenotype in in distinct manners and probably at different light intensities. When assessing interactions between the plasmotype and duplication effect in the DEPI dataset, no significant outcome was obtained in any of the time points (except for 3 time points in qI), suggesting that overall plasmotype and copy number effects on NPQ related parameters are additive. Additive genetic effects correspond to the phenotypic variance induced by independent contributions of two or more genes[74], in this case genetic factors underlying duplication and plasmotype effects. It implies that both effects can contribute to qE, NPQ, qI or Φ_{PSII} separately, without interfering with each other or altering the outcome of the final phenotype. This may be explained by the fact that no obvious antagonistic or synergistic effects were found to be present throughout the DEPI treatment (except for qE in constant light), allowing duplication and plasmotype effects to be examined separately (*Figure 9* B & C).

Duplicated *PnsL1* is a likely candidate to be responsible for the duplication effects on NPQ because of its involvement in NDH dependent CEF[51,52,54]. Potentially, higher *PnsL1* expression might result in increased NDH activity, which would impact the NPQ phenotype. On the other hand, the phenotypic variations caused by the plasmotype effect, might be attributable to another genetic factor involving NDH, which differs between the C24 and Bur plasmotypes. The Bur plasmotype, in fact, happens to have a unique missense mutation in the chloroplastic gene *NAD(P)H – QUINONE OXIDOREDUCTASE SUBUNIT 6* (*NdhG*)[41]. NdhG is a NDH subunit that, along with other chloroplast encoded components (NdhA to NdhG), forms one of the NDH membrane subcomplexes with H^+ pump activity[47,75]. Previous research on the impact of the missense mutation in CEF has confirmed that carrying the Bur plasmotype results in lower NDH activity[76]. This indicates that the *NdhG* allelic variation in Bur causes deficient protein functioning, which probably reduces total NDH H^+ pump activity. H^+ pumping is essential for NDH to be able to reduce PQ, which is a critical step in ensuring CEF continuity[77]. As a result, it could be postulated that *NdhG* mutation may result in decreased CEF rate. Therefore, duplication and plasmotype effects are most likely mediated by distinct mechanisms connected to NDH dependent CEF. The duplication effect might be boosting CEF while the Bur plasmotype would lower it, which would explain why their combination in $dBur^{Bur}$ results in milder NPQ phenotypic differences when compared to Bur-0 (*Figure 8* C).

Concluding, the study of the DEPI dataset has enabled to describe the dBur photosynthetic phenotype under different light settings, unveiling the inherent effect of two genetic factors that were addressed with consequent experiments.

4.2 Implication of *PnsL1* in the distinctive photosynthesis phenotype of dBur

One of the main outcomes of this project has been the characterisation of existing phenotypic divergences in NPQ caused by a nuclear locus duplication in dBur (*Figure 9* B). From a total 83 genes belonging to the duplicated region in chromosome 2, *PnsL1* is a likely candidate driving these differential adaptations because its involvement in CEF. Supposedly, the overexpression of *PnsL1* might have a boosting effect in NDH activity, which in turn could be influencing NPQ. Hence, the second goal of this thesis focused on finding evidence of a link between *PnsL1* expression and the dBur phenotype.

Via qPCR it was confirmed that *PnsL1* is certainly overexpressed in dBur cybrids (*Figure 11*). Furthermore, it was demonstrated that an increase in light intensity has no effect on the regulation of *PnsL1* expression (*Figure 12*). Biologically, this suggests that the possible effect of *PnsL1* overexpression involves a long-term effect, rather than a quick expression response to changing light circumstances. The light-dependent, highly variable phenotype detected in dBur does not rule out this hypothesis, since NDH activity is a very dynamic feature with a complicated participation in photosynthetic physiology that is largely reliant on the environment[53].

Thanks to the expression analysis, it was established that *PnsL1* duplication is associated with alterations in photosynthetic phenotype. As part of the NDH complex, overexpression of *PnsL1* may be producing increased NDH activity that could be accountable for the detected differences. However, it seems improbable that the duplication of a single gene, being a component of a highly conserved complex composed of more than 30 proteins[47,53,55], is capable of increasing overall NDH efficiency. The only reason this could be feasible is that *PnsL1* is a pivotal gene for the effective functioning of the complex, acting as a bottleneck for its viability. *PnsL1* has been proven to be indispensable for NDH complex accumulation in the thylakoid membranes due to its role in the stabilization of the NDH-PSI supercomplex formation[51,52,54]. Consequently, presence of *PnsL1* may be essential for the proper functioning of the NDH dependent CEF, as impaired protein function results in deficient NDH activity[54]. It may be a possibility that *PnsL1*, which is required to "anchor" NDH to PSI, could be able to favour NDH-PSI supercomplex formation when found in more abundance, resulting in enhanced NDH activity. Nonetheless, even though *PnsL1* overexpression is correlated with the distinctive phenotype observed in dBur, there is insufficient evidence to attribute causation. It is worth noting that *PnsL1* is not the only gene essential for NDH functioning. Many other complex subunits have also been proven to be fundamental for the viability of the complex, such as *Ndh*O or *NdhM* [47,51,77] (*Figure 3*). Hence, even though *PnsL1* is a promising candidate due to its role, there is not enough proof to claim it is a critical gene in NDH functioning. In order to assess the implication of *PnsL1* in the dBur phenotype with more consistency, further experimentation is needed.

To confirm that the *PnsL1* duplication is behind the dBur phenotype establishment of mutant lines is required. Over-expression of *PnsL1* in both Bur-WT and sBur (as well as Columbia), followed by a phenotypic comparison with dBur, should be a straightforward procedure to test this. Another possibility would be to use the CRISPR/Cas9 technique to supress a single *PnsL1* copy in dBur and assess whether the phenotype is equivalent to their homologues lacking the locus duplication. In this project, development of KO constructs for such experimentation was attempted leading to unsuccessful results. Main problematics concerning the cloning efforts included obtaining of low plasmid concentrations and few transformant colonies in the latter stages of the cloning process. Given that the plasmid purification technique applied has already been perfectioned by research staff in our lab and proven to be a reliable method in other experimental settings, it is probable that there could be an issue with the bacteria used. Perhaps the selected transformant colonies did not contain the recombinant plasmid, suggesting that

there could be a contamination problem[78]. Before proceeding with the cloning work, the used Mach1 *E.coli* cells should be double checked by plating them on LB-Agar plates containing Carbenicillin (100 µg/mL) and Spectinomycin (50 µg/mL) to guarantee that no bacterial growth is found.

4.3 Induction of the locus duplication phenotypic effect in the Robin

The third research question postulated in this study was whether higher NDH dependent CEF might be the cause for the distinctive photosynthetic performance reported in the Bur plants with the locus duplication. To address whether divergent NPQ dBur phenotype was associated with higher CEF via NDH complex, phenotyping experiments were conducted in plants grown under constant and fluctuating light conditions. First and foremost, these assays sought to determine if the NPQ phenotype found in the DEPI could be induced in our facilities. The evaluation of the NPQ traits in dBur cybrids utilizing the Robin led to results that could be related to the phenotype found in the DEPI system on multiple occurrences. In other situations, however, the findings did not correspond entirely.

When measuring qE after 200 µmol photons m^{-2} s^{-1} on the first day of the DEPI treatment (constant or "flat" day), the C24 plasmotype shows considerably greater qE (6-14%) than the Bur plasmotype (*Figure 9* B). Under the same conditions, there is no duplication effect (*Figure 9* C), which again suggests that the plasmotype (*NdhG*) is playing parlty different role than the duplication (*PnsL1*). A similar trend is found in the Robin, where measuring qE at 200 µmol photons m^{-2} s^{-1} in plants grown in constant light settings (n = 6) leads to a non-significant rise in qE in due to the duplication (*Supplementary Figure 2* E). Note that in the Robin the plasmotype effect can be perceived too, as $dBur^{C24}$ seems to have greater qE than $dBur^{Bur}$, and $sBur^{C24}$ appears to be over $sBur^{Bur}$ (*Supplementary Figure 2* E). The lack of significant plasmotypic divergence might be attributed to the fact that the plasmotype effect in the DEPI flat day does not arise until 3 h after exposure to 200 µmol photons m^{-2} s^{-1}. The Robin measurements, on the other hand, were conducted in the first hour in the morning and only lasted about 30 minutes. This suggests that the phenotype may take some time to emerge, meaning that there was insufficient waiting time to trigger significant plasmotypic differences. Additionally, it is worth noting this qE pattern resembles the one identified in the Robin after 200 µmol photons m^{-2} s^{-1} in plants receiving fluctuating light (n = 11) (*Figure 13* E), which does result in significant differences. It is also possible that the small number of plant replicates in constant light conditions is insufficient to detect these significant variations (n = 6 vs. n = 11). The Robin assays were planned to be completed in a single day. Including the same plant replicates in both treatments made this impossible due to the small number of plants that could be phenotyped at a time (20) and the long duration of the phenotyping protocol (40 minutes in total). Moreover, because photoprotection especially is critical upon fluctuating light, analysing NPQ and NDH under these circumstances was prioritised.

The decreasing duplication effects in NPQ reported on the first day of the DEPI system (*Figure 9* C) could not be identified in the Robin in plants receiving constant light treatment (*Supplementary Figure 2* C). As with qE, this most likely occurs because of the timing component, as the duplication does not result in lower NPQ until 8 hours after light exposure.

When it comes to the DEPI fluctuating day, when measurements are conducted in the low light (LL) periods (when light intensity is around 200-250 µmol photons m^{-2} s^{-1}), the C24 plasmotype exhibits increased qE relative to Bur (*Figure 9* B). This impact may be reflected in the plants receiving fluctuating light treatment when measured in the Robin as well. When qE is measured after 200 µmol photons m^{-2} s^{-1}, there is a considerable increasing effect not only caused by the duplication, but also by the C24 plasmotype (*Figure 13* E). $dBur^{C24}$ shows to have greater qE than $dBur^{Bur}$. $sBur^{C24}$ has higher qE than $sBur^{Bur}$ as well, although it does not vary statistically from Bur-WT. The plasmotypic effect can also be found in qI values obtained in the Robin in such conditions (*Figure 13* G). dBur lines show qI reduced values, but the presence of the C24 plasmotype prevents photoinhibition more efficiently. Looking at the DEPI data at the beginning of the fluctuation day (200-250 µmol photons m^{-2} s^{-1}), both the

duplication and the plasmotype have negative effects in qI (*Figure 9* B, *Figure 10* B), which is in line with our findings. Regarding NPQ, increasing effects of the duplication in the DEPI fluctuation setting (*Figure 10* B) only become obvious at LL periods of 300-500 µmol photons m^{-2} s^{-1}, conditions that were not tested in the Robin. In our setting measuring NPQ at 200 µmol photons m^{-2} s^{-1} results in a negative duplication effect in plants that received light fluctuation (*Figure 13* C). This also occurs in the DEPI system, since at the start of the fluctuations, when light is 200 µmol photons m^{-2} s^{-1}, NPQ is in fact 5% lower in the lines with the locus duplication (*Figure 10* B). From the results obtained in the high light (HL) periods in the DEPI fluctuation, the duplication shows to have a lowering impact on qE during 62 - 65h when the light intensity increases from 700 (-10%) to 1000 (-5%) µmol photons m^{-2} s^{-1} (*Figure 10* B). The negative effect size of the duplication does not fade until strong light is exposed for prolonged periods of time. This may explain why, when measured in the Robin, the cybrids with duplication have lower qE after application of HL (1000 µmol photons m^{-2} s^{-1}) (*Figure 13* F). Total NPQ on the other hand, does not appear to be influenced by the duplication upon DEPI HL (*Figure 10* B). This contradicts the Robin's findings, since dBur cybrids exhibited lower NPQ when tested after 1000 µmol photons m^{-2} s^{-1}, both in plants receiving constant and fluctuating light treatments (*Figure 13* D, *Supplementary Figure 2* D). Same occurs with qI. While in HL in DEPI appears to cause a continuous increase in qI in the plants with the locus duplication (*Figure 10* B), in our settings the effect is right the opposite (*Figure 13* H). Finally, when measuring with HL in the Robin an increasing duplication effect in Φ_{PSII} was detected in dBur plants receiving fluctuation treatment (*Figure 13* B). This impact could not be detected in the DEPI data. In fact, prolonged exposure to fluctuations happened to decrease Φ_{PSII} (*Figure 10* B).

The discrepancies between the two datasets might be attributed to a variety of factors. In the DEPI system, all plants are brought into the measuring facilities and allowed a day to acclimatize prior to measurements. Because the Robin is not a high-throughput system, transportation of the plants and 30-minute dark adaptation was required prior to measurements. As a result, the NPQ phenotype can be potentially influenced by plant acclimation responses. Furthermore, the DEPI method enables tracking the progression of photosynthetic parameters in real time. This is especially beneficial to study fluctuation effects, as light changes can occur gradually while the phenotype is monitored. In the Robin light shifts from 200 to 1000 µmol photons m^{-2} s^{-1} occur significantly faster, which may have different physiological consequences. This might be the reason for the observed disparities in NPQ and qI in plants treated with variable light, as abrupt changes in light intensity may not cause the expected NPQ or qI increase, while steady transitions to high light can. Moreover, there are a few concerns in comparing DEPI fluctuation to plants treated with oscillating light treatment in our study. In the Robin, real-time monitoring of NPQ under variable light was not possible. Instead, 5 days of fluctuating light treatment was applied prior to the measurements. This was done under the assumption that the genetic factors causing the known physiological differences would have a rather constant effect on the phenotype. Therefore, longer subjection to fluctuation would result in a constitutively larger NPQ, similar to the one detected in the DEPI. However, the divergent dBur NPQ phenotype has shown to be very changeable and strongly reliant on light conditions and exposure time. For this reason, to investigate this trait in a more reproducible manner, a static camera system allowing high throughput monitoring would be preferable.

In summary, although the dBur phenotype assessed in the Robin did not entirely correspond to the one characterised in the DEPI system, it was confirmed that differences in the photosynthetic phenotype owing to the duplication were indeed inducible in the Robin. Moreover, the distinct impact of the C24 plasmotype over the Bur plasmotype described in the DEPI data (*Figure 9* B) could be detected in the Robin too (*Figure* 13 E). In accordance with the DEPI analysis, assessment of interactions between the plasmotype and copy number yielded the same results. No significant interactions were found, supporting the existence of additive genetic effects that could be evaluated individually. The analysis of both datasets revealed that differentiating plasmotype effects arise at 200 µmol photons m^{-2} s^{-1} and are mostly associated with qE. Because qE is the NPQ component that is directly activated by ΔpH increase in the lumen[33,35–37], it might be possible that the found divergencies between plasmotypes are due to the *NdhG* mutation in the Bur plasmotype, which causes a decrease in NDH complex H^+ pump activity[76].

When it comes to the influence of the duplication, both DEPI and Robin results showed that its relevance becomes prominent at higher light intensities. In the DEPI dataset, increasing duplication effects on NPQ, qE and qI are at their peak around 500 µmol photons m^{-2} s^{-1} when prolonged fluctuations are applied (*Figure 10* B). The Robin results on the other hand show that short application of 1000 µmol photons m^{-2} s^{-1} has the opposite effect, as NPQ, qE and qI are reduced in dBur (*Figure 13* D, F & H). But most importantly, the duplication seems to maintain Φ_{PSII} levels higher when light is rapidly switched to stronger intensities (*Figure 13* B). After 1 minute of exposure to 1000 µmol photons m^{-2} s^{-1}, Φ_{PSII} $dBur^{Bur}$ is up to 10% greater than in $sBur^{Bur}$ ($p < 0.0001$), whereas in $dBur^{C24}$ it is about 7% higher than in $sBur^{C24}$ ($p = 0.0069$). This is especially interesting, as capacity to hold higher Φ_{PSII} upon abrupt exposure to high light might contribute to greater photosynthetic efficiency, which could result in biomass increase[79]. Notwithstanding, the DEPI data shows that extended subjection to light fluctuations can have the opposite effect in Φ_{PSII}, as it is relatively reduced due to the duplication (3-4% decrease, *Figure 10* B). The outcome of both DEPI and Robin studies indicate that the consequences of the duplication are very intricate and strongly reliant on the light environment. This suggests that the duplication, potentially via *PnsL1*, is influencing a complex photosynthetic regulatory system, possibly through increased NDH activity.

4.4 The link between NDH activity & NPQ and its biological relevance

After validating in the Robin that it was possible to induce differences in the photosynthetic phenotype owing to the duplication, the latter study focused on assessing whether the detected differences in Φ_{PSII} or NPQ related parameters could be linked to higher NDH activity in dBur.

The study of NDH activity under constant light conditions revealed that the plasmotypic effect is certainly present, since cybrids carrying the C24 plasmotype showed increased NDH activity compared to the Bur plasmotype (*Figure 15* Constant). The duplication effect can also be observed, with $dBur^{C24}$ showing higher activity than $sBur^{C24}$. Under these conditions, both copy number ($p = 0.033$) and plasmotype ($p < 0.0001$) effects are significant. Nonetheless, similar to the NPQ related phenotypes, interactions between plasmotype and copy number are not significant ($p = 0.15893$), indicating that their influence on NDH activity under constant light is additive. Exposure to fluctuating light, on the other hand, uncovers an intriguing occurrence. Increased NDH activity is only observed in $dBur^{C24}$, whilst $sBur^{C24}$ is no different from Bur-WT (*Figure 15* Fluctuating light). Yet plasmotype effects are still significant ($p < 0.0001$), just like the copy nr. ($p < 0.0001$). Interestingly, the interaction between the two components is significant in this situation ($p = 0.006$), showing the presence of epistatic effects. A significant interaction between copy number and plasmotype effects involves the existence of a functional association[80] influencing NDH activity. The notion that the duplication effect is only noticeable in the presence of the C24 plasmotype insinuates that there may be an interplay between the plasmotype and the duplication, which in turn affects the efficiency of the NDH complex under fluctuating light.

The fact that no significant differences in the NDH phenotype were found between $sBur^{Bur}$ and $dBur^{Bur}$ does not exclude the hypothesis that the duplication has an increasing effect in NDH activity. It is important to consider that NDH activity is measured in the dark, meaning that it is an indicative measurement. Hence, failing to detect higher NDH activity in $dBur^{Bur}$ in darkness does not directly imply that the duplication is not affecting NDH in the light, when photosynthesis is active. Hence, the duplication effect might just be masked, possibly by the Bur plasmotype. Deficient NDH activity caused by impaired *NdhG* function is a plausible explanation for the inability to find any differences in the NDH between $sBur^{Bur}$ and $dBur^{Bur}$. The *NdhG* mutation can affect total NDH activity under both constant and fluctuating light conditions. From the combination of the DEPI and Robin data, it can be deduced that the plasmotype effects have a more evident influence on the photosynthetic phenotype under constant/lower light intensities (200 µmol photons m^{-2} s^{-1}). Copy number and plasmotype effects are

found to be additive under these circumstances, which means that the independent effects may cancel each other out. Focusing on NDH activity when light is fluctuated, it may be postulated that the duplication impact becomes more relevant; yet the epistatic interaction with the Bur plasmotype obscures the boosting effect of the duplication in NDH activity. The opposite impact of *NdhG* and the duplication, potentially induced by increased expression of *PnsL1*, could indicate the existence of a cytonuclear interaction that is highly reliant on the light conditions. Epistatic interplay among genes can be very varied and highly dependent on the environment[80–82], which may explain why the interaction is found to be irrelevant in constant light settings.

Answering the final research question, phenotyping experiments have demonstrated that the duplication is indeed responsible for increased NDH dependent CEF. Despite the fact that no significant increase NDH activity could be detected in $dBur^{Bur}$, finding a clear difference between $dBur^{C24}$ and $sBur^{C24}$ strongly suggests that the duplication is indeed responsible for increased NDH activity (*Figure* 15). Therefore, higher NDH activity is definitively linked to differences in Φ_{PSII}, NPQ, qE and qI caused by the dBur locus duplication (*Figure* 13). How increased NDH complex activity might be mediating these changes in photosynthetic parameters, on the other hand, is a more challenging subject to address.

The reality is that the physiological relevance of NDH mediated CEF, including its role in photoprotection, is a very controversial topic that is yet to be deciphered. As a CEF pathway, NDH receives electrons from PSI and recycles them into the chain by pumping H^+ in the lumen (*Figure 1*). Consequently, it enables regeneration of $NADP^+$ and increases ATP/NADPH ratio to meet the ATP demand of the Calvin-Benson cycle[77]. As a result, NDH plays a protective role by limiting NADPH accumulation under supersaturating conditions, preventing build-up of harmful reactive intermediates[83].

However, the relationship between the NDH complex and the ΔpH-induced NPQ under stressful conditions is still not well stablished. Previously it has been demonstrated in *Arabidopsis* mutants with high CEF (*hcef*) that when the Calvin-Benson cycle is constitutively disrupted, NDH has the ability to q_E[84]. Other studies conducted with NDH-deficient mutants in several species have found evidence of sensitivity to strong light[85] and diverse abiotic stresses[86–88]. The mutants though, showed very mild phenotypes, and no impairment in NPQ induction[50]. Clear phenotypic effects of NDH dysfunctionality in growth and photosynthesis are especially perceived when PGR5-PGRL1 protein dependent CEF pathway is also defective[50]. These double mutants show decreased p700 oxidation ratio and electron transport rate even at very low light intensity[50]. Because of this reason, NDH dependent CEF has been proposed to act as a "safety valve", relieving oxidative stress upon conditions that cause severe reduction of chloroplast stroma such as low temperatures or fluctuating light[47,48,85–89]. Under these conditions, NDH dependent CEF is required for alleviating photodamage in both photosystems, principally by preventing overexcitation of PSI, which eventually leads to overall collapse of the electron transport chain[53,90].

Upon fluctuating light, abrupt increases in light intensity stimulate immediate induction of CEF, which is crucial for avoiding photoinhibition[90,91]. In the Robin experiments, when plants receiving fluctuating light treatment were subjected to a short period of high light (HL), it was discovered that, even though HL reduced overall Φ_{PSII} (*Figure 13* B, note that y axis differs), dBur cybrids were still able to maintain higher Φ_{PSII} and prevent photoinhibition (*Figure 13* H). Concomitantly, reduced qE and NPQ were observed. This might imply that, after a brief exposure to HL, the constitutively enhanced CEF via the NDH complex acts as a buffer against a sudden burst of electrons, allowing the correct electron flow to continue. As a result, by limiting electron build-up across the chain, improvement of NDH complex efficiency could actually be preventing photoinhibition and increasing Φ_{PSII} (*Figure* 16).

Conversely, it is conceivable that this beneficial effect is merely temporary, and that prolonged exposure to HL may be deleterious to total photosynthetic efficiency. In the DEPI data, when plants are exposed to oscillating light for an entire day, the duplication appears to have a relative decreasing effect on NPQ at the start of the fluctuations (*Figure 9* C, *Figure 10* B), which is consistent with the previously stated

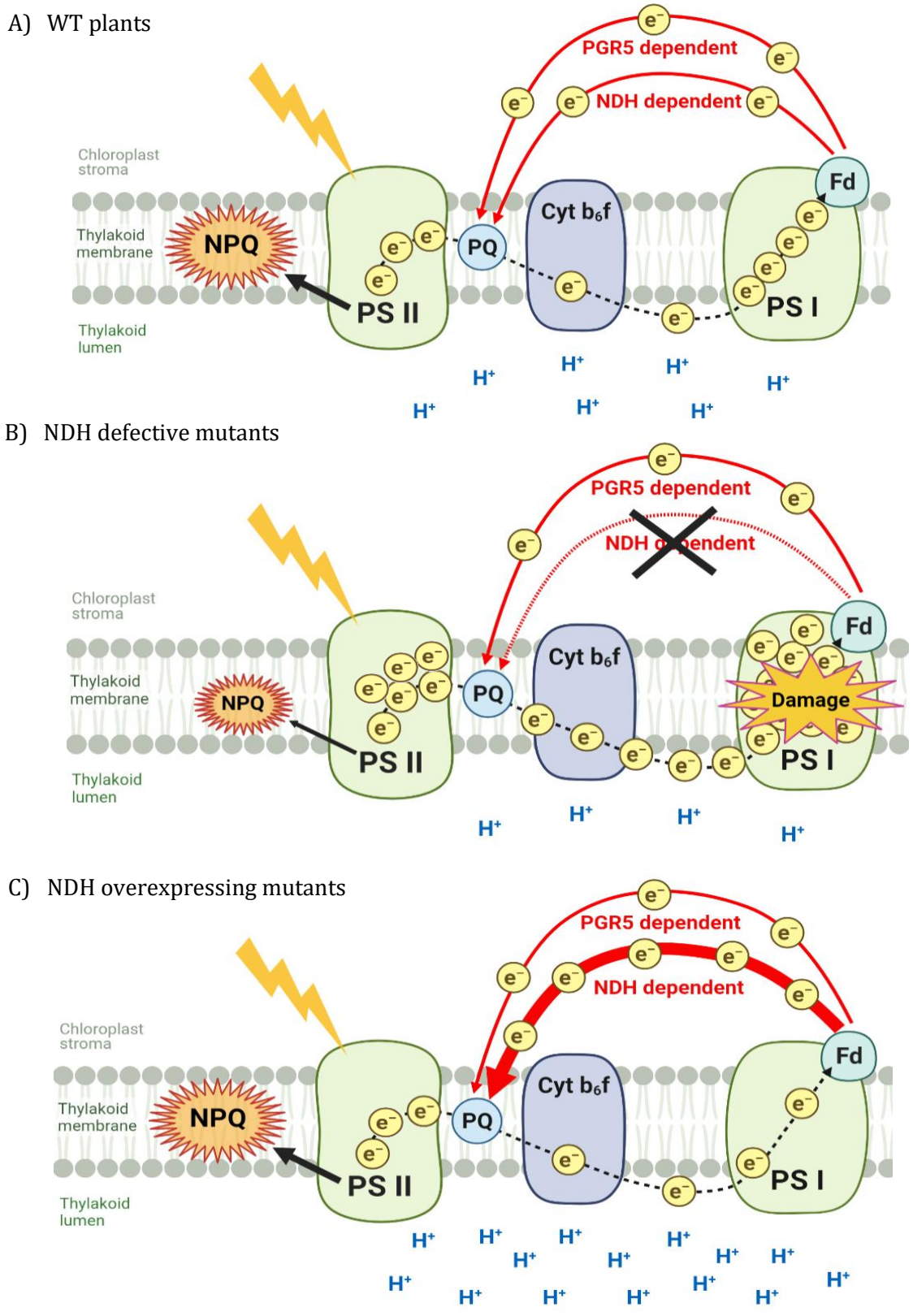

Figure 16 **| NDH-dependent CEF and its photoprotective role preventing photodamage.** Upon fluctuating light or sudden changes from low to high light, NDH complex could protect the photosynthetic machinery by avoiding the accumulation of electrons throughout the chain. A) In wild-type plants, high light supply causes the accumulation of reducing power in the electron transfer system, promoting CEF activity and NPQ activation through H^+ build-up in the lumen. B) In NDH defective mutants, CEF rate drops, which leads to over-reduction and damage at PSI first. Decrease in H^+ reduces NPQ and excess of energy can no longer be dissipated, causing over-accumulation of electrons in the system. C)Enhanced NDH activity in overexpressing mutants might increase overall photosynthetic efficiency by improved electron transfer rate. Long subjection to high light intensity might be necessary to raise ΔpH enough to boost NPQ. NPQ: Non-photochemical quenching, PSI/II: Photosystem I/II, PQ: Plastoquinone, Cyt *b6f*: Cytochrome *b6f* complex, Fd: Ferredoxin, e^-: electron, H^+: proton. Figure inspired by [90]

theory. When subjected to light variation over an extended amount of time, no differences due to the duplication were detected in the HL periods. After transitioning to LL though, plants containing the duplication showed to have relatively larger NPQ when light intensity was between 300-500 µmol photons m^{-2} s^{-1}. This might indicate that, during the 8 minutes of HL, NPQ induction is no different in dBur. However, upon shifting to LL phase, it is possible that NDH activity is stimulated in an attempt to reduce oxidative stress generated by HL exposure, depositing H^+ in the lumen and impeding NPQ relaxation. In line with this, monitoring photosynthetic efficiency under fluctuating light in NDH deficient rice *crr6* mutants revealed that in the low light phase of the oscillations NPQ, electron transport rate and CO_2 assimilation were reduced[90]. On the other hand, gradual increase of light intensity during the sinusoidal day resulted in substantially greater NPQ in dBur at 300-500 µmol photons m^{-2} s^{-1} (*Figure 9* C). In this situation, it might be possible that persistent exposure to raising light could provide enough time for enhanced NDH to elevate ΔpH, thereby activating NPQ. However, the present hypothesis does not explain why long-term subjection to raising or fluctuating light results in higher qI in plants containing the duplication (*Figure 10* B). Despite the fact that larger qI does not affect Φ_{PSII} in the sinusoidal day (*Figure 9* C), subjection to fluctuations does reduce Φ_{PSII} by 4% in the presence of the duplication. This is certainly a paradoxical outcome, as higher CEF is associated with less photoinhibition[91].

In addition to reducing oxidative stress in intense or variable light, NDH driven CEF has proven to be particularly relevant in low light (200 µmol photons m^{-2} s^{-1})[92–94]. Studies have shown that failure in NDH function in rice *crr6* mutants results in decreased CEF and NPQ when grown in low light conditions[92]. Similarly, in *Arabidopsis* mutants with deficient NDH activity (*crr4-2*) the magnitude of the proton motive force is decreased [95]. Accordingly, measurement of NDH activity in the Robin revealed that NDH activity was prominent under constant/low light settings (*Figure 15*). Moderate acidification by higher CEF through the NDH complex might explain why under these circumstances a mild increase in qE was found (*Figure 13* E). Because light reactions limit photosynthesis at low light intensity, NDH dependent CEF may be necessary to energize photosynthesis in such circumstances. Under sub-saturating light conditions, NDH dependent CEF may be able to regulate the redox state of the intermediate electron carriers and generate additional H^+ gradient to ensure correct ATP supply[92]. Furthermore, it has been demonstrated that photoinhibition of PSII stimulates CEF and increases p700 oxidation under low light[93], lending credence to the photoprotective function of NDH being active in sub-saturating conditions. As a result, low-light activation of CEF primarily enhances ATP production, which is required for PSII to operate efficiently[94]. This might explain why, in the DEPI system, dBur exhibits higher Φ_{PSII} (%1) in constant/low light setting (*Figure 9* C*)*.

The possibility of improving photosynthetic efficiency sets hopeful prospects to boost crop production[4,96,97]. Improving the efficiency of light reactions by modulation of NDH dependent CEF may contribute to this goal. As a dynamic electron transmitter, it can safeguard photosystems from damage caused by HL or variable light. As a highly efficient proton pump, it increases the amount of ATP produced and balance ATP/NADPH budget, which can boost photosynthetic efficiency under both high and low light circumstances. However, the consequent increase in H^+ for greater ATP synthesis might come at a cost, as by exacerbating ΔpH NPQ is triggered, which constrains the overall photochemical reactions[77].

The pertinent question is whether overexpression of a gene like *PnsL1*, which may result in greater CEF via NDH, would be beneficial to improve yield. The combination of phenotyping experiments carried out in this project with the analysis of previously collected data has enabled to determine that the photosynthetic phenotype caused by potentially higher NDH activity is more variable than expected, very dependent on the light environment and subjection time to specific light conditions. The duplication appears to modestly favour photosynthetic efficiency in constant/low light conditions (%1) (*Figure 9* C). Same occurs upon abrupt changes from LL to HL where Φ_{PSII} is found to be 7-10% higher in the dBur lines (*Figure 13* B). On the other hand, Φ_{PSII} is decreased up to 4% due to duplication when plants are subjected to longer fluctuations (*Figure 10* B). Nevertheless, in order to assess the relevance

of the reported variation in photosynthetic efficiency and be able to discern fast adaptation mechanisms from desirable long-term effects, the impact of the duplication on plant biomass should be examined under different light environments.

Previous research has demonstrated that under fluctuating light, impairment of NDH complex in *crr6* mutants lead to photoinhibition of PSI, decline in photosynthetic rate and consequent reduction of CO_2 assimilation and biomass production[90]. Experiments in *Arabidopsis ndhO* and *ndhM* mutants, as well as cybrids bearing the *NdhG* defective Bur plasmotype, have also revealed that exposure to severe light fluctuation has a detrimental effect on vegetative growth[76]. Likewise, disruption of the NDH function in rice under constant low light circumstances, resulted in significant reduction of CO_2 assimilation rate with concomitant decay in biomass and grain production[92].

Because NDH deficient mutants exhibit decreased tolerance against photo-oxidative stress, over-expression of NDH subunits may enable breeding of stress-tolerant plants. Furthermore, NDH over-expression can aid in the development of new C4 crop varieties, as NDH functioning is essential to supply the ATP demand of the carbon concentrating C4 metabolism[98]. Alternatively, improving NDH dependent CEF might contribute to crop productivity gains in places where light is scarce[92], or in artificial environments where light expenses must be reduced, such as vertical farms.

Nonetheless, the fact that NDH is a highly conserved complex across photosynthetic organisms should not be disregarded[53]. Being such a large complex, it is probable that any beneficial mutation by duplication or deletion of any of its components would have already been selected throughout evolution (assuming that higher photosynthetic efficiency is selected upon). This might imply that there is very little room for improvement. Yet, genetic modification of the complex may still result in desirable features that are beneficial for farming in particular settings but do not explicitly entail better fitness. The key here is to determine the trade-off that will enable future targeted breeding to address the imminent increase in food demand.

5. CONCLUSIONS & RECOMMENDATIONS

Completion of the current project enabled the validation that the nuclear locus duplication present in $dBur^{Bur}$ and $dBur^{C24}$ leads to divergencies in photosynthetic traits. Characterization of the dBur phenotype revealed that the consequences of the duplication are not limited to a constitutively increased NPQ as previously expected. Instead, the close examination of the DEPI system's time series phenotypic data showed that the photosynthetic phenotype of dBur is very variable and light intensity dependent. Additionally, it was found that the phenotype is not only affected by the duplication, but also the plasmotype. The quantification of the *PnsL1* expression in constant and sinusoidal light settings verified the *PnsL1* duplication, indicating that over-expression of *PnsL1* is correlated with the dBur phenotype. Besides, it demonstrated that gene expression is not influenced by rising light intensity, implying that the potential gene function effect is constitutive rather than a quick expression response to light increase. Phenotyping experiments confirmed that the differences in photosynthetic parameters caused by the duplication are reproducible in the Robin. It was reported that upon fast transitions from low to high light, NPQ, qE and qI are lowered due to duplication, resulting in higher Φ_{PSII}. Finally, phenotypic dissimilarities between dBur and sBur showed to be relatable to differences in NDH activity under both constant and high/fluctuating light conditions. Relevance of the plasmotype in NDH activity was described in low light, whereas nuclear locus duplication exposed its importance in both fluctuating light and quick shifts from low to high light.

The detailed characterisation of the dBur phenotype achieved throughout this project lays the groundwork for future research into the role of the candidate gene *PnsL1* in NPQ and overall photosynthetic efficiency. The response of the dBur traits to different light conditions and intensities when measured in the Robin has been established. Now, it is time to apply the gained knowledge to evaluate *PnsL1* KO and overexpression Bur mutants under such settings. Furthermore, the influence of the duplication in biomass production should be examined in different light environments to assess the biological relevance of the reported phenomena.

The physiological significance of the NDH complex is still undetermined and many steps must be taken to unveil its comprehensive role in photosynthesis. As a very large and well conserved protein complex its biological relevance should not be disregarded. Further efforts are necessary to uncover how tuning of NDH dependent CEF may contribute to breeding crop varieties with increased yield through optimized photosynthesis.

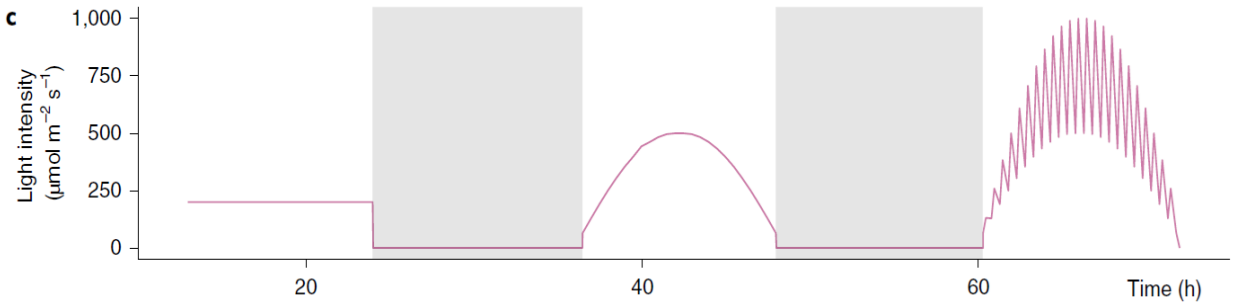

Supplementary Figure 1 | DEPI light system from Michigan State University. Three consecutive days are depicted, with constant (day 1), sinusoidal (day 2) and fluctuating light intensity (day 3). Nights are represented by grey shaded areas. Picture obtained from [41].

AL | 200 µmol photons m^{-2} s^{-1} **HL | 1000 µmol photons m^{-2} s^{-1}**

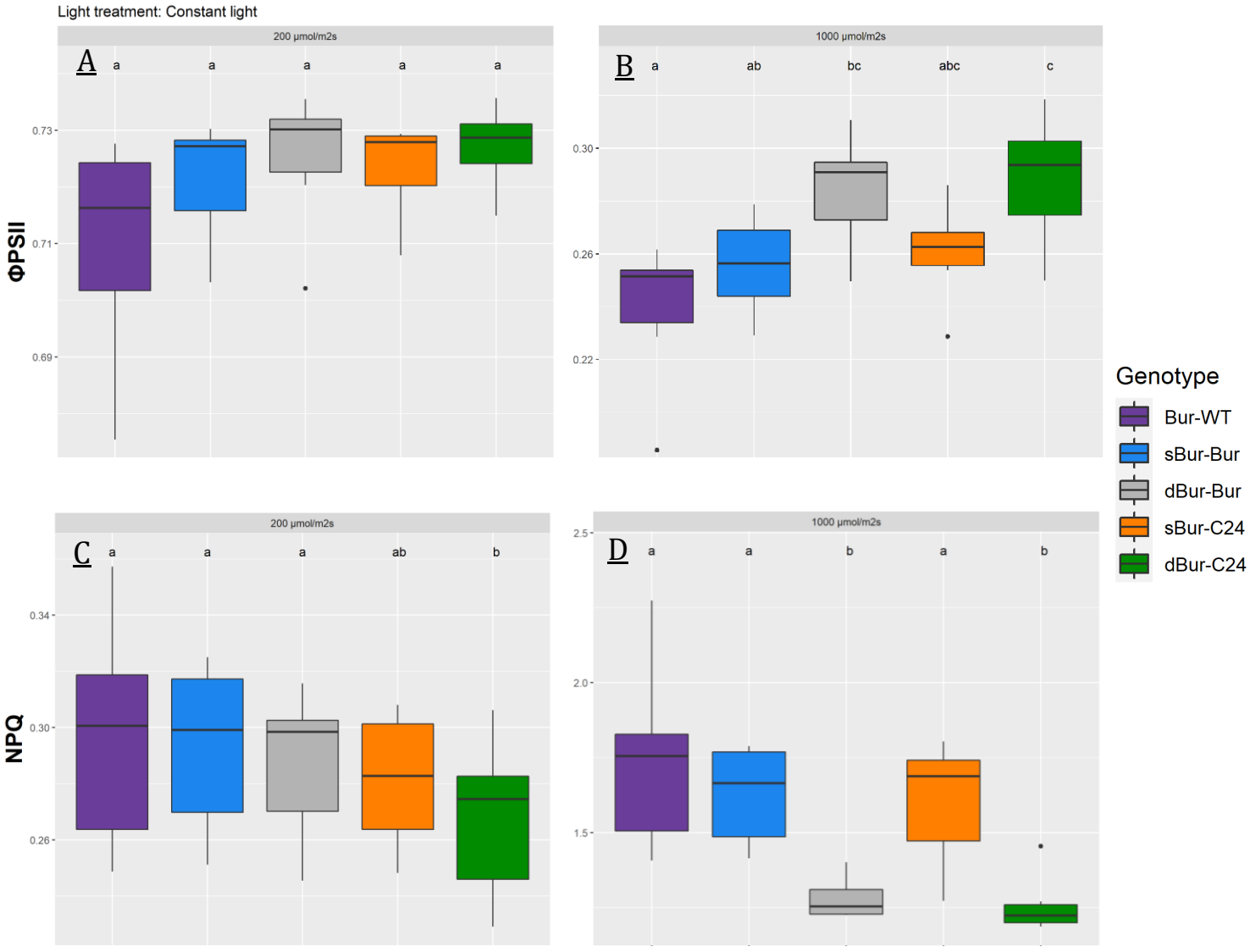

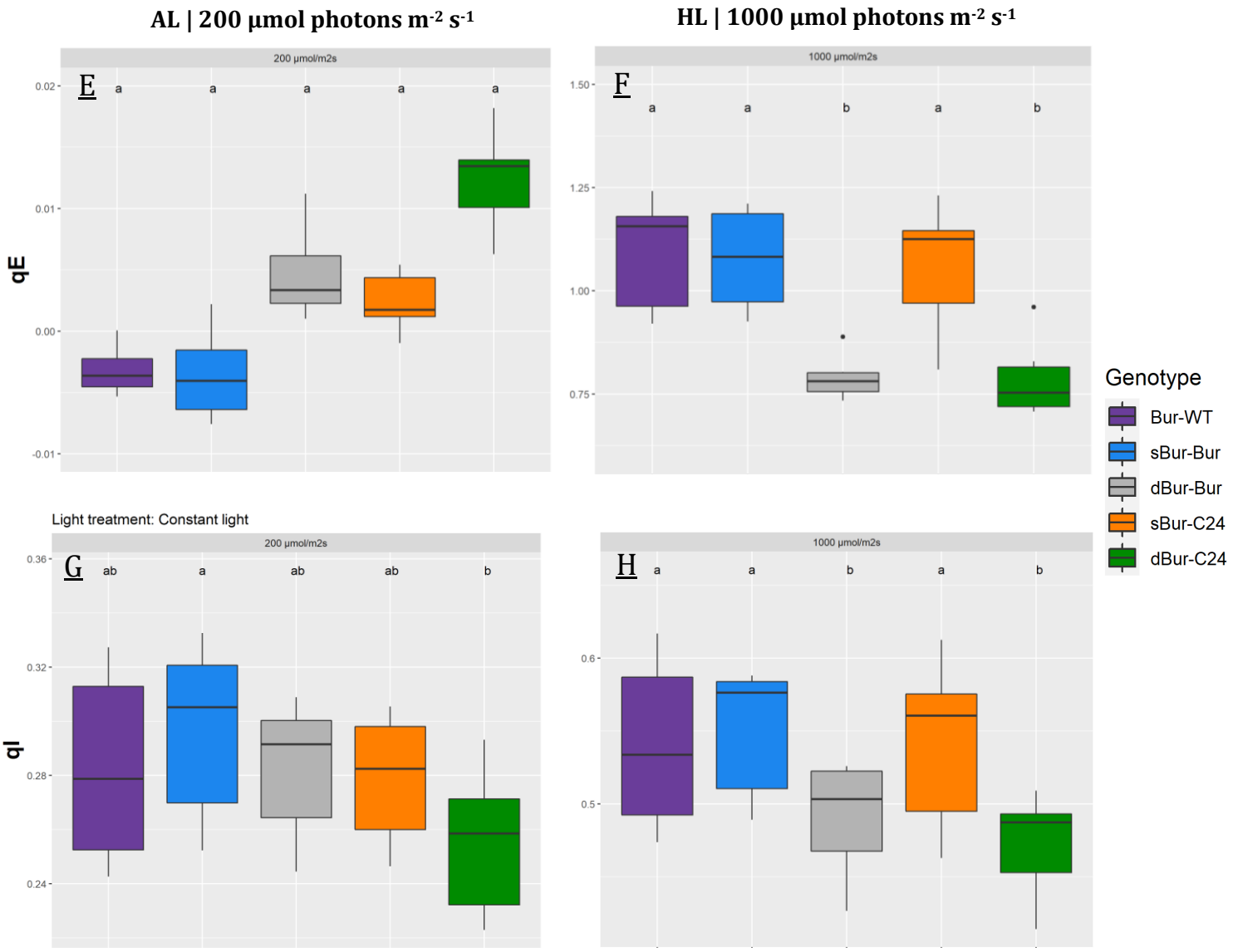

***Supplementary Figure 2*| Photosynthetic performance of Bur-WT and Bur cybrids.** *Arabidopsis thaliana* Burren-0 wild-type (Bur-WT) and cybrids containing nuclear locus duplication ($dBur^{Bur}$ and $dBur^{C24}$) as well as a single copy of the locus ($sBur^{Bur}$ and $sBur^{C24}$), receiving the constant light treatment (n = 6). Cybrid genotypes in the legend are denoted as double/single nucleotype-plasmotype. Light intensity applied to infer photosynthetic parameters is displayed at the top of the plot columns, low light (LL, 200 µmol photons m^{-2} s^{-1}) and high light (HL, 1000 µmol photons m^{-2} s^{-1}). Φ_{PSII} refers to the efficiency of photosystem II under applied light conditions, measured as $(F_m'-F_p)/F_m'$. NPQ represents the photochemical quenching of light energy surplus activated as a protection mechanism against high light, estimated as $F_m/F_m' - 1$. qE is the fast NPQ component triggered by H^+ accumulation in the lumen, inferred as $(F_m/F_m') - (F_m/F_m'')$. qI represents the photoinhibitory NPQ occurring when Φ_{PSII} is damaged, calculated as $(F_m'- F_m'')/ F_m''$. See section 2.2 in Materials & Methods for further explication of the calculations. Boxes represent interquartile ranges with medians (black horizontal line) + spread of the data (whiskers). Note that scales in y axes differ per plot. Different letters on top of the boxes represent statistically significant differences across genotypes ($p < 0.05$).

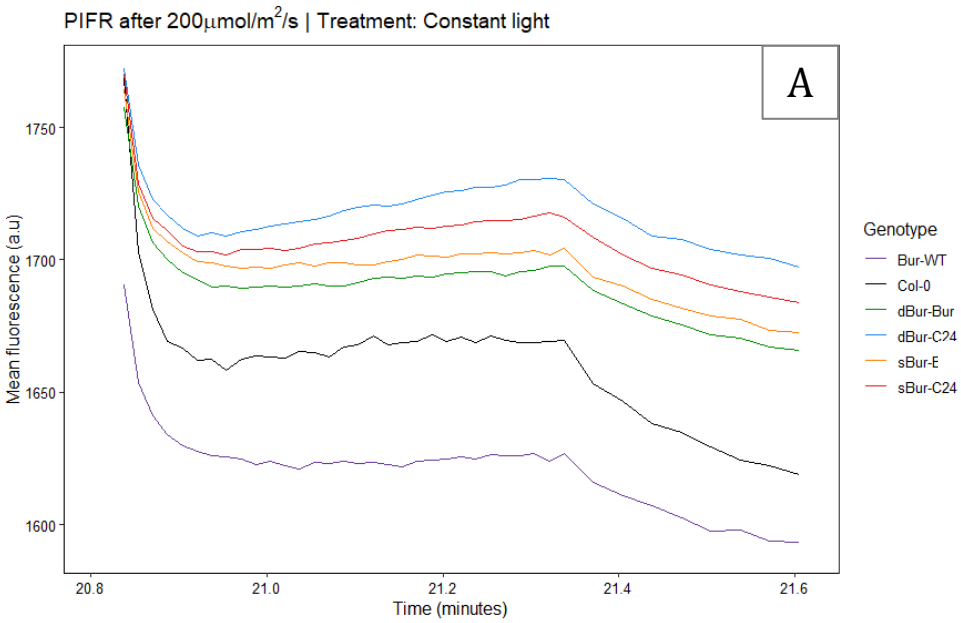

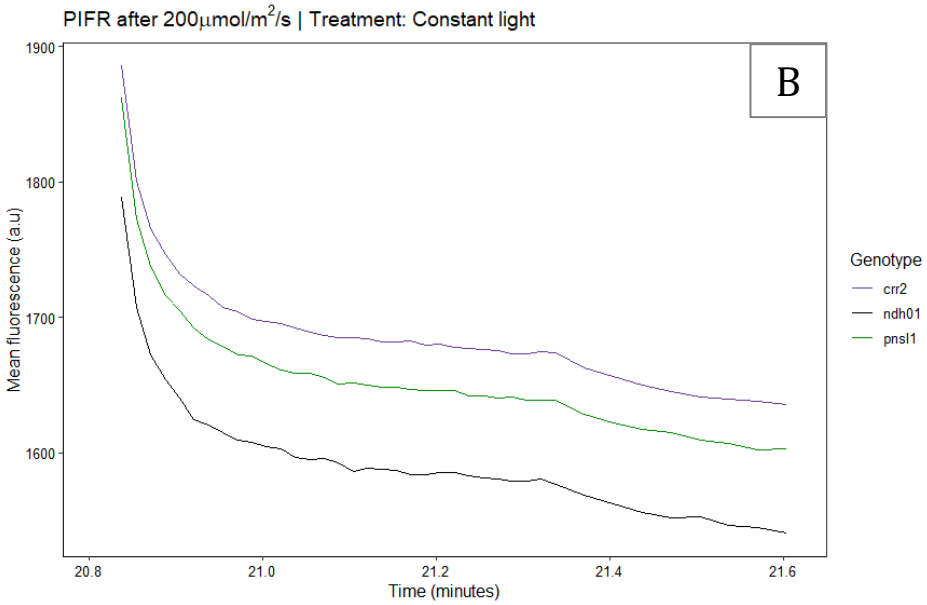

Supplementary Figure 3 **| Post illumination fluorescence increase (PIFR)** monitored in the dark after application of 200 µmol m^{-2} s^{-1} in plants receiving constant light treatment. **A)** *Arabidopsis thaliana* Col-0 and Burren wild-type (Bur-WT) and cybrids containing nuclear locus duplication ($dBur^{Bur}$ and $dBur^{C24}$) as well as a single copy of the locus ($sBur^{Bur}$ and $sBur^{C24}$). **B)** *A. thaliana* Columbia NDH defective mutants *crr2*, *ndh0* and *pnsl1*. Lines represent genotypic fluorescence means. Y axis corresponds to raw fluorescence values (arbitrary units, a.u.). X axis depicts time (minutes).

REFERENCES

1. Hohmann-Marriott, M. F. & Blankenship, R. E. Evolution of Photosynthesis. *http://dx.doi.org/10.1146/annurev-arplant-042110-103811* **62**, 515–548 (2011).
2. Long, S. P., Zhu, X.-G., Naidu, S. L. & Ort, D. R. Can improvement in photosynthesis increase crop yields? *Plant. Cell Environ.* **29**, 315–330 (2006).
3. Taylor, S. H. & Long, S. P. Slow induction of photosynthesis on shade to sun transitions in wheat may cost at least 21% of productivity. *Philos. Trans. R. Soc. B Biol. Sci.* **372**, (2017).
4. Ort, D. R. *et al.* Redesigning photosynthesis to sustainably meet global food and bioenergy demand. *Proc. Natl. Acad. Sci.* **112**, 8529–8536 (2015).
5. Zhu, X. G., Long, S. P. & Ort, D. R. What is the maximum efficiency with which photosynthesis can convert solar energy into biomass? *Curr. Opin. Biotechnol.* **19**, 153–159 (2008).
6. Zhu, X.-G., Ort, D. R., Parry, M. A. J. & von Caemmerer, S. A wish list for synthetic biology in photosynthesis research. *J. Exp. Bot.* **71**, 2219–2225 (2020).
7. Ruban, A. V. Evolution under the sun: optimizing light harvesting in photosynthesis. *J. Exp. Bot.* **66**, 7–23 (2015).
8. Kromdijk, J. *et al.* Improving photosynthesis and crop productivity by accelerating recovery from photoprotection. *Science (80-.).* **354**, 857–861 (2016).
9. Murchie, E. H. & Niyogi, K. K. Manipulation of Photoprotection to Improve Plant Photosynthesis. *Plant Physiol.* **155**, 86–92 (2011).
10. Long, S. P., Humphries, S. & Falkowski, P. G. Photoinhibition of photosynthesis in nature. *Annu. Rev. Plant Biol.* **45**, 633–662 (1994).
11. Werner, C., Ryel, R. J., Correia, O. & Beyschlag, W. Effects of photoinhibition on whole-plant carbon gain assessed with a photosynthesis model. *Plant. Cell Environ.* **24**, 27–40 (2001).
12. Zhu, X., Ort, D. R., Whitmarsh, J. & Long, S. P. The slow reversibility of photosystem II thermal energy dissipation on transfer from high to low light may cause large losses in carbon gain by crop canopies: a theoretical analysis. *J. Exp. Bot.* **55**, 1167–1175 (2004).
13. Garcia-Molina, A. & Leister, D. Accelerated relaxation of photoprotection impairs biomass accumulation in Arabidopsis. *Nat. Plants 2020 61* **6**, 9–12 (2020).
14. Demmig-adams, B., Cohu, C. M., Stewart, J. J. & Iii, W. W. A. *Non-Photochemical Quenching and Energy Dissipation in Plants, Algae and Cyanobacteria*. *Photosynthesis and Respiration* vol. 40 (2014).
15. Blankenship, R. E. Molecular Mechanisms of Photosynthesis. in p 312 (Wiley Blackwell, London, 2014).
16. Ort, D. R. & Yocum, C. F. *Oxygenic photosynthesis: the light reactions*. vol. 4 (Springer Science & Business Media, 1996).
17. Walker, B. J., Kramer, D. M., Fisher, N. & Fu, X. Flexibility in the Energy Balancing Network of Photosynthesis Enables Safe Operation under Changing Environmental Conditions. *Plants 2020, Vol. 9, Page 301* **9**, 301 (2020).
18. Joliot, P. & Johnson, G. N. Regulation of cyclic and linear electron flow in higher plants. *Proc. Natl. Acad. Sci.* **108**, 13317–13322 (2011).
19. Johnson, G. N. Physiology of PSI cyclic electron transport in higher plants. *Biochim. Biophys. Acta - Bioenerg.* **1807**, 384–389 (2011).

20. Nawrocki, W. J. *et al.* The mechanism of cyclic electron flow. *Biochim. Biophys. Acta - Bioenerg.* **1860**, 433–438 (2019).

21. Joliot, P., Joliot, A. & Johnson, G. Cyclic electron transfer around photosystem I Photosystem I: The Light-Driven Plastocyanin: Ferredoxin Oxidoreductase ed JH Golbeck. (2006).

22. Allen, J. F. Cyclic, pseudocyclic and noncyclic photophosphorylation: new links in the chain. *Trends Plant Sci.* **8**, 15–19 (2003).

23. Heber, U. & Walker, D. Concerning a Dual Function of Coupled Cyclic Electron Transport in Leaves. *Plant Physiol.* **100**, 1621–1626 (1992).

24. Makino, A., Miyake, C. & Yokota, A. Physiological Functions of the Water–Water Cycle (Mehler Reaction) and the Cyclic Electron Flow around PSI in Rice Leaves. *Plant Cell Physiol.* **43**, 1017–1026 (2002).

25. Ort, D. R. When There Is Too Much Light. *Plant Physiol.* **125**, 29–32 (2001).

26. Melis, A. Photosystem-II damage and repair cycle in chloroplasts: what modulates the rate of photodamage in vivo? *Trends Plant Sci.* **4**, 130–135 (1999).

27. Niyogi, K. K. Safety valves for photosynthesis. *Curr. Opin. Plant Biol.* **3**, 455–460 (2000).

28. Ort, D. R. & Baker, N. R. A photoprotective role for O2 as an alternative electron sink in photosynthesis? *Curr. Opin. Plant Biol.* **5**, 193–198 (2002).

29. Asada, K. The water-water cycle in chloroplasts: scavenging of active oxygens and dissipation of excess photons. *Annu. Rev. Plant Biol.* **50**, 601–639 (1999).

30. Powles, S. B. Photoinhibition of photosynthesis induced by visible light. *Annu. Rev. Plant Physiol.* **35**, 15–44 (1984).

31. Nixon, P. J., Michoux, F., Yu, J., Boehm, M. & Komenda, J. Recent advances in understanding the assembly and repair of photosystem II. *Ann. Bot.* **106**, 1–16 (2010).

32. Vass, I. Molecular mechanisms of photodamage in the Photosystem II complex. *Biochim. Biophys. Acta (BBA)-Bioenergetics* **1817**, 209–217 (2012).

33. Ruban, A. V & Wilson, S. The Mechanism of Non-Photochemical Quenching in Plants: Localization and Driving Forces. *Plant Cell Physiol.* **00**, 1–10 (2020).

34. Tikkanen, M., Rantala, S. & Aro, E.-M. Electron flow from PSII to PSI under high light is controlled by PGR5 but not by PSBS. *Front. Plant Sci.* **6**, 521 (2015).

35. Rees, D., Young, A., Noctor, G., Britton, G. & Horton, P. Enhancement of the ΔpH-dependent dissipation of excitation energy in spinach chloroplasts by light-activation: correlation with the synthesis of zeaxanthin. *FEBS Lett.* **256**, 85–90 (1989).

36. Noctor, G., Rees, D., Young, A. & Horton, P. The relationship between zeaxanthin, energy-dependent quenching of chlorophyll fluorescence, and trans-thylakoid pH gradient in isolated chloroplasts. *Biochim. Biophys. Acta (BBA)-Bioenergetics* **1057**, 320–330 (1991).

37. Kiss, A. Z., Ruban, A. V. & Horton, P. The PsbS protein controls the organization of the photosystem II antenna in higher plant thylakoid membranes. *J. Biol. Chem.* **283**, 3972–3978 (2008).

38. Krause, G. H. Photoinhibition of photosynthesis. An evaluation of damaging and protective mechanisms. *Physiol. Plant.* **74**, 566–574 (1988).

39. Kress, E. & Jahns, P. The Dynamics of Energy Dissipation and Xanthophyll Conversion in Arabidopsis Indicate an Indirect Photoprotective Role of Zeaxanthin in Slowly Inducible and Relaxing Components of Non-photochemical Quenching of Excitation Energy. *Front. Plant Sci.* **8**, 2094 (2017).

40. Pérez-Bueno, M. L., Johnson, M. P., Zia, A., Ruban, A. V. & Horton, P. The Lhcb protein and xanthophyll composition of the light harvesting antenna controls the ΔpH-dependency of non-photochemical quenching in Arabidopsis thaliana. *FEBS Lett.* **582**, 1477–1482 (2008).

41. Flood, P. J. *et al.* Reciprocal cybrids reveal how organellar genomes affect plant phenotypes. *Nat. Plants* **6**, 13–21 (2020).

42. Ravi, M. *et al.* A haploid genetics toolbox for Arabidopsis thaliana. *Nat. Commun. 2014 51* **5**, 1–8 (2014).

43. Ravi, M. & Chan, S. W. L. Haploid plants produced by centromere-mediated genome elimination. *Nat. 2010 4647288* **464**, 615–618 (2010).

44. Cruz, J. A. *et al.* Dynamic Environmental Photosynthetic Imaging Reveals Emergent Phenotypes. *Cell Syst.* **2**, 365–377 (2016).

45. Ohno, S. *Evolution by gene duplication*. (Springer Science & Business Media, 2013).

46. Hallinid, J. & Landryid, C. R. Regulation plays a multifaceted role in the retention of gene duplicates. (2019) doi:10.1371/journal.pbio.3000519.

47. Shikanai, T. Chloroplast NDH: A different enzyme with a structure similar to that of respiratory NADH dehydrogenase. *Biochim. Biophys. Acta - Bioenerg.* **1857**, 1015–1022 (2016).

48. Kouřil, R. *et al.* Structural characterization of a plant photosystem i and NAD(P)H dehydrogenase supercomplex. *Plant J.* **77**, 568–576 (2014).

49. Shikanai, T. Regulatory network of proton motive force: contribution of cyclic electron transport around photosystem I. *Photosynth. Res. 2016 1293* **129**, 253–260 (2016).

50. Munekage, Y. *et al.* Cyclic electron flow around photosystem I is essential for photosynthesis. *Nat. 2004 4296991* **429**, 579–582 (2004).

51. Peng, L., Fukao, Y., Fujiwara, M., Takami, T. & Shikanai, T. Efficient operation of NAD(P)H dehydrogenase requires supercomplex formation with photosystem I via minor LHCI in arabidopsis. *Plant Cell* **21**, 3623–3640 (2009).

52. Otani, T., Kato, Y. & Shikanai, T. Specific substitutions of light-harvesting complex I proteins associated with photosystem I are required for supercomplex formation with chloroplast NADH dehydrogenase-like complex. *Plant J.* **94**, 122–130 (2018).

53. Strand, D. D., D'Andrea, L. & Bock, R. The plastid NAD(P)H dehydrogenase-like complex: structure, function and evolutionary dynamics. *Biochem. J.* **476**, 2743–2756 (2019).

54. Ishihara, S. *et al.* Distinct Functions for the Two PsbP-Like Proteins PPL1 and PPL2 in the Chloroplast Thylakoid Lumen of Arabidopsis. *Plant Physiol.* **145**, 668–679 (2007).

55. Kato, Y., Sugimoto, K. & Shikanai, T. NDH-PSI Supercomplex Assembly Precedes Full Assembly of the NDH Complex in Chloroplast. *Plant Physiol.* **176**, 1728 (2018).

56. Hashimoto, M., Endo, T., Peltier, G., Tasaka, M. & Shikanai, T. A nucleus-encoded factor, CRR2, is essential for the expression of chloroplast ndhB in Arabidopsis. *Plant J.* **36**, 541–549 (2003).

57. Searle, S. R., Casella, G. & McCulloch, C. Variance Components. *Wiley, New York* (1992).

58. Patterson, H. D. & Thompson, R. Recovery of Inter-Block Information when Block Sizes are Unequal. *Biometrika* **58**, 545 (1971).

59. Bates, D., Sarkar, D., Bates, M. D. & Matrix, L. The lme4 package. *R Packag. version* **2**, 74 (2007).

60. Lenth, R. V. emmeans: Estimated Marginal Means, aka Lest-Squares Means. R package version 1.6.3. *https://CRAN.R-project.org/package=emmeans.* (2021).

61. Czechowski, T., Stitt, M., Altmann, T., Udvardi, M. K. & Scheible, W. R. Genome-Wide

Identification and Testing of Superior Reference Genes for Transcript Normalization in Arabidopsis. *Plant Physiol.* **139**, 5–17 (2005).

62. Livak, K. J. & Schmittgen, T. D. Analysis of Relative Gene Expression Data Using Real-Time Quantitative PCR and the 2−ΔΔCT Method. *Methods* **25**, 402–408 (2001).

63. Jinek, M. *et al.* A Programmable Dual-RNA – Guided. **337**, 816–822 (2012).

64. Engler, C. *et al.* A golden gate modular cloning toolbox for plants. *ACS Synth. Biol.* **3**, 839–843 (2014).

65. Concordet, J. P. & Haeussler, M. CRISPOR: Intuitive guide selection for CRISPR/Cas9 genome editing experiments and screens. *Nucleic Acids Res.* **46**, W242–W245 (2018).

66. Ordon, J. *et al.* Generation of chromosomal deletions in dicotyledonous plants employing a user-friendly genome editing toolkit. *Plant J.* **89**, 155–168 (2017).

67. Stuttmann, J. *et al.* Highly efficient multiplex editing: one-shot generation of 8× Nicotiana benthamiana and 12× Arabidopsis mutants. *Plant J.* **106**, 8–22 (2021).

68. Russell., J. F. S. and D. W. Molecular Cloning: A Laboratory Manual, Ed 3. *New York Cold Spring Harb. Lab. Press* (2001).

69. Bimboim, H. C. & Doly, J. A rapid alkaline extraction procedure for screening recombinant plasmid DNA. *Nucleic Acids Res.* **7**, 1513 (1979).

70. Schreiber, U. Pulse-amplitude-modulation (PAM) fluorometry and saturation pulse method: an overview. *Chlorophyll a Fluoresc.* 279–319 (2004).

71. Otani, T., Yamamoto, H. & Shikanai, T. Stromal Loop of Lhca6 is Responsible for the Linker Function Required for the NDH–PSI Supercomplex Formation. *Plant Cell Physiol.* **58**, 851–861 (2017).

72. Schreiber, U., Klughammer, C. & Walz, H. Complementary PS II quantum yields calculated from simple fluorescence parameters measured by PAM fluorometry and the Saturation Pulse method. **1**, (2008).

73. Ruban, A. V. Nonphotochemical Chlorophyll Fluorescence Quenching: Mechanism and Effectiveness in Protecting Plants from Photodamage. *Plant Physiol.* **170**, 1903–1916 (2016).

74. Rieger, R., Michaelis, A. & Green, M. M. *A Glossary of Genetics and Cytogenetics: Classical and molecular*. *New York: Springer-Verlag* (New York: Springer-Verlag, 1968). doi:10.1007/978-3-662-01012-9.

75. Laughlin, T. G., Bayne, A. N., Trempe, J.-F., Savage, D. F. & Davies, K. M. Structure of the complex I-like molecule NDH of oxygenic photosynthesis. *Nat. 2019 5667744* **566**, 411–414 (2019).

76. Theeuwen, T. P. J. M. Allelic variation in chloroplastic ndhG reveals role for NDH complex in more dynamic photosynthesis. *[Unpublished manuscript]* (2022).

77. Strand, D. D., Fisher, N. & Kramer, D. M. The higher plant plastid NAD(P)H dehydrogenase-like complex (NDH) is a high efficiency proton pump that increases ATP production by cyclic electron flow. *J. Biol. Chem.* **292**, 11850–11860 (2017).

78. Troubleshooting Guide for Cloning | NEB. https://international.neb.com/tools-and-resources/troubleshooting-guides/troubleshooting-guide-for-cloning.

79. Huang, M. *et al.* Leaf photosynthetic performance related to higher radiation use efficiency and grain yield in hybrid rice. *F. Crop. Res.* **193**, 87–93 (2016).

80. Moore, J. H. *Gene Interaction*. *Brenner's Encyclopedia of Genetics: Second Edition* (Academic Press, 2013). doi:10.1016/B978-0-12-374984-0.00592-1.

81. Kerwin, R. E. *et al.* Epistasis × environment interactions among Arabidopsis thaliana

glucosinolate genes impact complex traits and fitness in the field. *New Phytol.* **215**, 1249–1263 (2017).

82. Jagdishchandra Joshi, C. & Prasad, A. Epistatic interactions among metabolic genes depend upon environmental conditions. *Mol. Biosyst.* **10**, 2578–2589 (2014).

83. Cruz, J. A. *et al.* Plasticity in light reactions of photosynthesis for energy production and photoprotection. *J. Exp. Bot.* **56**, 395–406 (2004).

84. Livingston, A. K., Cruz, J. A., Kohzuma, K., Dhingra, A. & Kramer, D. M. An Arabidopsis Mutant with High Cyclic Electron Flow around Photosystem I (hcef) Involving the NADPH Dehydrogenase Complex. *Plant Cell* **22**, 221–233 (2012).

85. T, E. *et al.* The role of chloroplastic NAD(P)H dehydrogenase in photoprotection. **457**, 5–8 (1999).

86. Munné-Bosch, S., Shikanai, T. & Asada, K. Enhanced ferredoxin-dependent cyclic electron flow around photosystem I and α-tocopherol quinone accumulation in water-stressed ndhB-inactivated tobacco mutants. *Planta* **222**, 502–511 (2005).

87. Yamori, W., Sakata, N., Suzuki, Y., Shikanai, T. & Makino, A. Cyclic electron flow around photosystem I via chloroplast NAD (P) H dehydrogenase (NDH) complex performs a significant physiological role during photosynthesis and plant growth at low temperature in rice. *Plant J.* **68**, 966–976 (2011).

88. Wang, P. *et al.* Chloroplastic NAD (P) H dehydrogenase in tobacco leaves functions in alleviation of oxidative damage caused by temperature stress. *Plant Physiol.* **141**, 465–474 (2006).

89. Shikanai, T. Cyclic Electron Transport Around Photosystem I: Genetic Approaches. *http://dx.doi.org/10.1146/annurev.arplant.58.091406.110525* **58**, 199–217 (2007).

90. Yamori, W., Makino, A. & Shikanai, T. A physiological role of cyclic electron transport around photosystem I in sustaining photosynthesis under fluctuating light in rice. *Sci. Reports 2016 61* **6**, 1–12 (2016).

91. Takahashi, S. *et al.* How Does Cyclic Electron Flow Alleviate Photoinhibition in Arabidopsis? *Plant Physiol.* **149**, 1560–1567 (2009).

92. Yamori, W., Shikanai, T. & Makino, A. Photosystem I cyclic electron flow via chloroplast NADH dehydrogenase-like complex performs a physiological role for photosynthesis at low light. *Sci. Rep.* **5**, 1–10 (2015).

93. Huang, W., Yang, Y. J., Hu, H. & Zhang, S. B. Different roles of cyclic electron flow around photosystem I under sub-saturating and saturating light intensities in tobacco leaves. *Front. Plant Sci.* **6**, 923 (2015).

94. Huang, W., Yang, Y. J., Zhang, S. B. & Liu, T. Cyclic Electron Flow around Photosystem I Promotes ATP Synthesis Possibly Helping the Rapid Repair of Photodamaged Photosystem II at Low Light. *Front. Plant Sci.* **9**, (2018).

95. Wang, C., Yamamoto, H. & Shikanai, T. Role of cyclic electron transport around photosystem I in regulating proton motive force. *Biochim. Biophys. Acta - Bioenerg.* **1847**, 931–938 (2015).

96. Yamori W. Improving Photosynthesis to Increase Food and Fuel Production by Biotechnological Strategies in Crops. *J Plant Biochem Physiol. J Plant Biochem Physiol* **1**, 113 (2013).

97. Long, S. P., Marshall-Colon, A. & Zhu, X. G. Meeting the global food demand of the future by engineering crop photosynthesis and yield potential. *Cell* **161**, 56–66 (2015).

98. Endo, T., Ishida, S., Ishikawa, N. & Sato, F. Chloroplastic NAD(P)H Dehydrogenase Complex and Cyclic Electron Transport around Photosystem I. *Plant Cell* **25**, 1–5 (2008).